THE MECHANISM OF BENEFICIAL EFFECTS OF BORON AND ZIRCONIUM ON CREEP-RUPTURE PROPERTIES OF A COMPLEX HEAT RESISTANT ALLOY

by
Raymond F. Decker

A dissertation submitted in partial fulfillment
of the requirements for the degree of
Doctor of Philosophy in the
University of Michigan
1957

Doctoral Committee:

Professor James W. Freeman, Chairman
Assistant Professor Wilbur C. Bigelow
Professor Lawrence O. Brockway
Professor Richard A. Flinn
Professor Lars Thomassen

THE MECHANISM OF BENEFICIAL EFFECTS OF BORON AND ZIRCONIUM ON CREEP-RUPTURE PROPERTIES OF A COMPLEX HEAT RESISTANT ALLOY

By Raymond F. Decker

A microstructural investigation was pursued to establish the mechanism of the pronounced benefits of boron and zirconium on creep-rupture properties of a 55 Ni - 20 Cr - 15 Co - 4 Mo - 3 Ti - 3 Al alloy at 1600°F.

Materials with varying boron and zirconium content were exposed to creep conditions and then the microstructures were analyzed by optical and electron microscopy, electron diffraction, microfractography and hardness measurements. Particularly useful were interrupted creep tests which allowed comparisons of materials after equivalent creep exposures.

The mechanism of improvement of creep-rupture properties was found to be a pronounced stabilizing effect of boron and zirconium on the grain boundaries of the alloy. The alloy with low boron and zirconium was subject to rapid agglomeration of $M_{23}C_6$ and γ' ($Ni_3(Al, Ti)$) in the grain boundaries, followed by depletion of γ' and intergranular micro-cracking at the grain boundaries transverse to applied stress. Brittle fracture then occurred by linking of micro-cracks. However, additions of zirconium, boron and boron plus zirconium decreased this tendency in that order. In the absence of these elements extensive micro-cracking was found early in second stage creep at relatively short time periods and fracture occurred prematurely with very little deformation. Proper amounts of boron plus zirconium delayed micro-cracking

until after third stage creep started so that creep-rupture life was greatly prolonged and ductility to fracture markedly increased.

No effect of the trace elements on the size, amount and distribution of the intragranular γ' was detected. Accordingly, the property effects were not found to result from a change in the intragranular γ' reaction.

An estimate of the generality and limitations of the mechanism is given in the report. It appears that the effect of boron and zirconium generally would be to retard agglomeration of phases in the grain boundaries of heat resistant alloys.

Consideration is given to the cause of the stabilizing influence of the trace elements. The most feasible explanation is equilibrium segregation of boron and zirconium to grain boundaries, lowering the energy level of the grain boundaries and thereby reducing the tendency for carbon segregation to the grain boundaries.

to
James Wright Freeman

PREFACE

It is a pleasure to acknowledge all those who aided in this investigation and particularly the following:

Professor J. W. Freeman, Chairman of the author's Doctoral Committee and supervisor of the sponsoring research project, for his patient tutoring, helpful suggestions and critical analyses during the course of the investigation.

Professors L. O. Brockway, R. A. Flinn and L. Thomassen, members of the Doctoral Committee, for helpful advice and cooperation.

Professor W. C. Bigelow and J. A. Amy, pioneers in the techniques and applications of microstructural examination of metals, for invaluable assistance in electron microscopy, electron diffraction and microfractography.

The National Advisory Committee for Aeronautics for sponsorship and financial assistance.

My fellow graduate students in Metallurgical Engineering and associates in the High Temperature Group for theoretical suggestions on the research program.

K. E. Kienholz, A. G. Dano, T. M. Cullen, G. R. Hynes, R. A. Umstead and Miss Christine Sadler of the High Temperature Group for assistance in the experimental program.

TABLE OF CONTENTS

LIST OF TABLES

LIST OF FIGURES

INTRODUCTION

High temperature properties of heat resistant alloys have been found to be sensitive to trace elements. This appears to be the source of marked heat-to-heat variations in creep-rupture properties obtained with an alloy of constant nominal chemical composition. The usual source of the trace elements leading to heat-to-heat variations is melting, either in selection of melting stock, through uncontrolled contamination of the melt by atmosphere or crucibles, or through "deoxidation" of the melt.

An example of trace element effects is found in recent studies of nickel base alloys hardened with titanium and aluminum. Boron[1,2,3,4*] and zirconium[1,2], introduced inadvertently from crucible contamination or purposefully in "deoxidation," markedly benefit creep-rupture properties. Cognizance of the effects has allowed producers to manufacture these alloys with properties consistently on the high side of previous scatter bands of creep-rupture properties.

Although progress has been made in correlating the creep-rupture properties of complex alloys with trace element content and in controlling trace element content to allow attainment of reproducible high properties from heat to heat, little has been established about the mechanisms of the pronounced effects on creep-rupture properties. Yet, it seems that establishment of mechanisms would be fruitful by increasing knowledge in theory of alloying for improving complex heat resistant alloys, perhaps even by revealing the nature of creep and fracture mechanism in these materials.

---

* The superscripts refer to literature listed under REFERENCES.

It is probable that the mechanisms involve the phase transformations of the alloy or other fine details of the alloy structure. This and the recent advances in microstructural techniques, including electron microscopy, microfractography and selected area electron diffraction, make a microstructural analysis a most promising method for detection of the mechanism.

For the above reasons, the objective of this study was to establish the mechanism of the beneficial effects of trace elements on the creep-rupture properties of a complex heat resistant alloy by a study of microstructures.

Since the marked effects of trace boron and zirconium on nickel base alloys are of great current interest, this mechanism was selected for study. A 55 Ni - 20 Cr - 15 Co - 4 Mo - 3 Ti - 3 Al alloy was chosen since creep-rupture properties had been correlated with trace element content in this material[1] and since stock was readily available.

REVIEW OF LITERATURE

Effects of Boron and Zirconium on Creep-Rupture Properties

A recent study[1] of effects of variable melting practice on heat-to-heat variations in properties of a 55 Ni - 20 Cr - 15 Co - 4 Mo - 3 Ti - 3 Al alloy indicated that introduction of trace boron or zirconium, inadvertently from crucible contamination or purposefully in "deoxidation," was the most important melting practice variable.

In summary, the findings were:

1. Creep-rupture life and ductility at 1600°F and 25,000 psi increased with boron content when zirconium was less than 0.01 percent (figs. 1 and 2).
2. Creep-rupture life and ductility at 1600°F and 25,000 psi increased with zirconium content when boron was less than 0.0005 percent (figs. 3 and 4).
3. The addition of 0.01 percent zirconium to material containing 0.009 percent boron raised both creep-rupture life and ductility significantly above the material with either element alone.
4. Minimum second stage creep rates were lowered slightly by zirconium and more markedly by boron (fig. 5).

Confirmation of these correlations on the commercial version of the alloy, Udimet 500, was obtained on boron by Koffler, Pennington and Richmond[2], Darmara[3] and Jones[4] and on zirconium by Koffler, Pennington and Richmond[2].

Literature on Relation of Properties to Microstructures

The literature on microstructures of nickel base alloys was reviewed to establish the state of knowledge on relations between creep-rupture properties and microstructure.

It is generally accepted that the major cause of the favorable high temperature properties of the Ti + Al hardened nickel base alloys is the precipitation of the intermetallic γ' phase within the matrix of the alloy. The γ' phase has been shown to have a face centered cubic structure similar to that of the Ni_3Al phase of the nickel-aluminum system with a lattice parameter closely matched to that of the matrix of the alloys[5,6]. Compositionally, the phase has been shown to dissolve titanium and is frequently referred to as $Ni_3(Al, Ti)$.

The creep resistance of these alloys has been attributed to the presence of γ'[5,7] and to the fact that γ' forms in fine dispersion within the matrix; however, attempts to relate the distribution of the γ' particles with the metallurgical properties have been only moderately successful to date. Frey, Freeman, and White[8] and subsequently Brockway and Bigelow[9] found that dispersion of the γ' particles before creep exposure in Inconel-X alloy correlated with creep-rupture properties at 1200°F, which was low in the aging range for this alloy; however, no correlation was obtained for rupture tests at 1500°F, which was high in the aging range. Betteridge and Smith[10] studied the effect on the creep-rupture properties of Nimonic alloys of variation in the amount and distribution of the γ'. Although it was established that highest creep-rupture properties were obtained with the greatest content of precipitated γ', some of the marked effects of heat treatment on creep-rupture properties could not be explained by changes in the

conditions of precipitation of γ'. In this case, the testing was relatively high in the aging range for γ'. Baillie[11] found that the most creep resistant Ni - Cr - Al - Ti alloys had the highest surface density of γ' particles (the number of particles per surface unit seen in electron micrographs). This corresponded to the smallest average spacing between particles and was in agreement with the theories of age hardening.

Recent microstructural studies indicated that the phase transformations in nickel base alloys are not restricted to γ'. Several carbide transformations have been identified, including those of $M_{23}C_6$[9, 12, 13], M_6C[12, 13], Cr_7C_3[14] and TiC[12, 13]. The occurrence of carbides is dependent both on the alloy composition and temperature of treatment. Marked tendencies have been found for precipitation in grain boundaries. The available literature indicates that the transformations are quite complex, involving transition phases and many instances where two or more of these carbides compete for the available carbon. Although carbide reactions in several commercial alloys have been thoroughly analyzed by microstructural techniques, little correlation has been made with creep-rupture properties. The potential of such correlations, however, is indicated by the success of Betteridge and Franklin[14] in relating creep-rupture life to the form and amount of Cr_7C_3 at the grain boundaries in Nimonic alloys.

Limited research on the effect of creep on microstructures of Ti + Al hardened nickel base alloys appears in the literature. This has been aimed at detecting creep damage and the cause for fracture. Baillie and Poulignier[15] did not find an effect of creep deformation on the dispersion of intragranular γ' but did detect a pronounced agglomeration at grain boundaries during creep. Mathieu[16] detected this agglomeration in jet engine blades removed from service and hypothesized that

the agglomerate was chromium carbides or nitrides and γ'.

In general, it was evident from the literature that moderate success had been met in relating properties to microstructure in nickel base alloys. Creep-rupture properties correlated with γ' dispersion under limited conditions, although in some cases no correlation was found. The work on carbide reactions and possible effects on properties emphasizes their importance. From this background information, it is apparent that careful microstructural analysis of the effect of boron or zirconium on the transformations of γ' and carbides might reveal the mechanism of beneficiation of creep-rupture properties.

EXPERIMENTAL PROCEDURES

The general procedure was to observe microstructural changes when materials with varying boron and zirconium content were subjected to thermal treatments involving temperature and stress. The experimental methods are described below.

Material

The experimental heats of the 55 Ni - 20 Cr - 15 Co - 4 Mo - 3 Ti - 3 Al alloy had been induction melted in the University of Michigan vacuum melting furnace. The heats were coded to indicate the relative boron and zirconium level; Heat V having low boron and zirconium, Heat V + Zr having relatively high zirconium, Heat V + B having relatively high boron and Heat V + B + Zr having significant content of both boron and zirconium. The virgin melting stock was electrolytic nickel, electrolytic chromium, electrolytic cobalt, arc-melted molybdenum, Ti 55A titanium, 99.99 percent aluminum pig, electrolytic manganese, 99.9 percent silicon powder and spectrographically pure carbon. Boron was added to Heats V + B and V + B + Zr as NiB. The zirconium contained in Heats V + Zr and V + B + Zr was derived from reaction with zirconia crucibles used in melting. Heat V was melted in an alumina crucible while Heat V + B was melted in magnesia.

The 10-pound ingots had been processed as follows:

1. Homogenized 1 hour at 2300°F, air cooled.
2. Surface ground.
3. Rolled to 7/8-inch bar stock from 2150°F; 22 passes, each of about 7-percent reduction in area, were used with 10-

minute reheats at 2150°F between passes.

Chemical analyses had been made on sections of the bar stock which originally were at the ingot center. In addition, material after creep exposure was checked for boron content. The results are listed in table I. Boron and zirconium were determined to be the only significant heat-to-heat variables. All the stock was homogenized 2 hours at 2150°F and air cooled prior to further experimentation.

Stress Aging and Creep-Rupture Testing

Treatments under stress were performed in stress-rupture units with strain measurements being made with an extensometer-mirror system with a sensitivity of 0.000005 inches per inch.

Solution treated bar stock was machined to 0.250-inch test specimens with a 1-inch gage section. A uniform time period of 4 hours of preheating at test temperature in the creep-rupture units was used before stress application. The stress aged samples were interrupted at the desired time by release of the load and immediate removal from the furnace.

Hardness

Diamond pyramid hardness (DPH) was measured with a 50-kilogram load. Three impressions were made on each sample, both diagonals of each impression being measured. Statistical analysis of testing variability established that in the range of 200 to 340 DPH a hardness difference of 7 DPH was significant while in the range of 340 to 400 DPH a hardness difference of 9 DPH was significant.

Metallography

Light Microscopy

Metallographic samples were mechanically polished through wet papers to 600 grit and then, with the majority, on wet cloths with Linde A and Linde B powders. A few, as noted in the figures, were electropolished after 600 grit paper in a solution of 10 parts of perchloric acid (70 percent) and 90 parts of glacial acetic acid at 30 volts with a current density of 2 amperes per square inch. Cyclic polishing of 5 seconds on and 5 seconds off was employed for a total period of electrolysis of 30 seconds.

The procedure and etchant developed by Bigelow, Amy and Brockway[17] was used to best reveal the precipitating phases at 100, 1000 and 2000 diameters. Etching was electrolytically at 6 volts and a current density of 0.8 amperes per square inch for periods of 5 to 7 seconds, depending upon the sample condition. The etchant composition was 12 parts of phosphoric acid (85 percent), 47 parts of sulfuric acid (96 percent) and 41 parts of nitric acid (70 percent).

The light micrographs are mounted with the rolling direction (and axis of tension in the case of creep specimens) vertical and in the plane of the figure.

Electron Microscopy

Metallographic samples were mechanically polished through wet papers to 600 grit. Following this was electropolishing with the procedure described in the previous section on light microscopy.

Etching for the electron microstructures was accomplished with the etchant described under light microscopy using 6 volts and a current

density of 0.8 amperes per square inch for periods of 1 to 5 seconds.

After etching, collodion replicas of the metallic surface were made. These were shadowed with palladium to increase contrast and reveal surface contours; polystyrene latex spheres of approximately 3400A in diameter were placed on the replicas prior to shadowing to indicate the angle and direction of shadowing and to provide an internal standard for measurement of magnification. The micrographs reproduced in this paper are copies of direct prints from the original negatives; consequently, the polystyrene spheres appear black and the "shadows" formed by the palladium appear white.

Orientation of electron micrographs in relation to rolling direction was not determined except where noted in the figures.

Counting Techniques

Depleted grain boundaries, micro-cracks, "nodules" (massive mixtures of γ' and carbides) and surface cracks were detected in this study. In order to make the trends and comparisons quantitative, counts were made of the number of each feature in the area traversed. In the case of depleted grain boundaries, micro-cracks and nodules, surveying was with an oil immersion lens at 1000 diameters on mechanically polished and etched specimens. An area of 0.008 square inches was covered, this being comprised of eight strips, each 0.2 inch by 0.005 inch. In the case of interrupted creep tests, the strips were longitudinal to the specimen axis at the center of the specimen and at the minimum cross section. In ruptured samples, the strips were again longitudinal, starting in the grains at the fracture surface and progressing away from the fracture. A depleted grain boundary was counted when a clear, white strip of matrix free of γ' particles was

clearly seen along a grain boundary. Micro-cracks were easily distinguishable by their blackness which was in complete contrast to all other intragranular and intergranular features of the samples. Early doubts about the identity were eliminated when electropolishing enlarged and accentuated these black voids and when fins on electron microscope replicas were found where these had filled the micro-cracks. Each distinct micro-crack was counted; 1 micron was selected as the minimum size counted since shorter micro-cracks were not distinguishable from carbide-matrix interfaces. Counting of nodules was arbitrarily limited to those above 5 microns in diameter.

Intergranular surface cracks were counted on mechanically polished creep specimens by traversing longitudinal section surfaces at 500 diameters. This cracking was found to be quite uniform over the reduced section of the specimens. In the case of interrupted creep specimens, the cracks were counted over the center 0.75 inches, while in ruptured samples, counts were made for 0.50 inches from the fracture. Intergranular cracks penetrating more than 0.003 inches deep were counted.

A measure of γ' dispersion was obtained by the surface density of γ' particles in electron microstructures. An area large enough to contain at least 100 particles was surveyed at 12,000 diameters.

The above techniques allow quantitative comparison of the tendency of the four heats to undergo the changes. It is recognized that percent of grain boundary area cracked, percent of grain boundary area depleted, volume percent of nodules, and volume percent and interparticle distance of γ' would be fundamentally more sound quantities for correlation. However, these more refined and time consuming

techniques would not alter the conclusions of this paper and, therefore, were not considered necessary.

Duplicate stress aged samples were run in several cases in order to give an estimation of the reproducibility of the microstructural changes and counting methods.

Electron Diffraction

The extraction-replica technique of Fisher[18] was used to permit identification of precipitating phases by electron diffraction.

Specimen Preparation

For extraction of intragranular γ', the specimen preparation was identical to the electropolishing and etching used for electron microscopy.

The specimen preparation for extraction of intragranular carbides consisted of electropolishing and then electrolytically etching for 15 minutes in 2 parts phosphoric acid (85 percent) to 8 parts water in order to remove γ'.

For extraction of intergranular particles, the microfractographic techniques of Plateau, Henry and Crussard[19] proved very useful. Specimens were cooled in liquid nitrogen and then fractured using a hammer and chisel, the fracture being intercrystalline. The fracture surface was then etched with the same procedure described above for electron microscopy.

Replication

Carbon replica films were deposited on the prepared surfaces by the method of Bradley[20] and were backed by thicker supporting

films of collodion. The surfaces were then etched electrolytically in a solution of 2 parts phosphoric acid (85 percent) to 8 parts water until the compound replica films separated from them. The films were transferred to the surface of clean distilled water and allowed to wash by diffusion, picked up on nickel screens, washed again, and the collodion backing films dissolved from the carbon films with amyl acetate by the method of Jaffe[21]. The replicas were then shadowed with aluminum to provide an internal standard for interplanar distances. Electron micrographs were obtained from the replicas in an RCA Model EML electron microscope. In addition, electron diffraction patterns were obtained from the particles by selected area electron diffraction techniques on the microscope.

Thermal Exposures Used Before Microstructural Examination

The four experimental heats were exposed to several treatments before microstructural examination. The exposures, purpose of each and limitations on comparison were:

1. No exposure, initial condition as solution treated 2 hours at 2150°F, air cooled - to detect differences in microstructure before creep exposure.
2. Aged 1/2, 1, 4, 10, 100, 188 and 500 hours at 1600°F - to show response of materials to temperature effects alone.
3. Stress aged 165 hours at 1600°F and 20,000 psi - to show response to creep exposures of equal stress and time (because of differing creep rates, as shown in figure 6, the total creep deformations were unequal).

4. Stress aged to rupture at 1600°F and 25,000 psi - to show response to creep exposures of equal stress (because of varying rupture life and ductility as shown in figure 7, the exposure times and total creep deformations were unequal).
5. Stress aged at 1600°F at stresses selected to give comparable time-elongation curves pictured in figure 8 - to compare response to creep exposures of equal strain, strain rate and time (because of varying creep strengths, the stresses were unequal as listed: Heat V - 20,000 psi, Heat V + Zr - 22,500 psi, Heat V + B - 28,000 psi, Heat V + B + Zr - 30,000 psi).

Details on stress aging conditions are listed in table II.

RESULTS

Marked microstructural changes occurred in Heat V during creep exposure at 1600°F. In terms of properties, the most significant changes were at the grain boundaries where a process of agglomeration of $M_{23}C_6$, depletion of γ' precipitates, micro-cracking and, finally, brittle fracture occurred. This process was retarded by zirconium, more by boron and most by boron with zirconium.

Other microstructural features developed during exposure at 1600°F, including intragranular carbide in the heats with boron, alignment of γ', intergranular surface cracking and nodular mixtures of carbides and γ'. The details of the grain boundary changes as well as other microstructural changes are given in the following sections.

Microstructures in Initial Condition

After the initial homogenizing treatment of 2 hours at 2150°F and air cooling, the experimental heats were similar in grain size (fig. 9), inclusion count and distribution (fig. 9), and grain boundary precipitate (figs. 10 and 11). Precipitation of γ' occurred during the air cooling after the 2150°F treatment. Some slight differences in dispersion of intragranular γ' existed but these were not found to be significant as discussed later. Hardnesses (fig. 9) did not differ significantly in this condition.

Changes in Microstructure During Exposure at 1600°F

Tables III and IV list the quantitative data on microstructural changes.

Agglomeration in Grain Boundaries

A network of carbides enveloped by γ' accumulated in the grain boundaries of all samples during exposure at 1600°F. In Heat V, the rate of accumulation was comparatively rapid, the carbide phase being extensive and blocky and the γ' layer thick after 165 hours exposure with 1.2 percent creep deformation (figs. 12, 13 and 14). The amount of agglomeration under these conditions was somewhat lower in Heat V + Zr and much lower in Heats V + B and V + B + Zr (figs. 13 and 14).

The agglomerated γ' was easily identified by etching characteristics. The agglomerate reacted to etching in the same manner as the intragranular γ' in all the experimental work carried out. It always was in the same relief and had the same appearance as the intragranular γ'.

Microfractographic techniques were used to identify the carbide phase and obtain more information on its form. Samples from Heats V and V + B after 1.2 percent creep deformation at 1600°F in 165 to 188 hours were cooled in liquid nitrogen and then fractured. Extraction replication from the fractured surface removed the grain boundary carbide and retained it in the replica. Electron micrographs showing the size and distribution of carbides in the grain boundaries are shown in figure 15. The extracted particles from Heat V were larger, more extensive and thicker than those from Heat V + B. The electron diffraction spots obtained on the replicas of the two samples indexed for $M_{23}C_6$.

Depletion of γ' at Grain Boundary

Subsequent to the agglomeration of $M_{23}C_6$ in the grain boundaries, strips of matrix were depleted of γ' particles along transverse grain

boundaries of the stress aged specimens (fig. 16). This occurred most often adjacent to $M_{23}C_6$ particles. This was in contrast to samples aged without stress, where the intergranular $M_{23}C_6$ was always enveloped by γ' and where the fine γ' particles extended up to the grain boundary (figs. 17 and 18).

In figure 16, the amount of this depletion is related to creep deformation for the experimental heats exposed to give equal strain at equal time at 1600°F. It is evident that boron and zirconium are effective in reducing the amount of this depletion with a given strain at 1600°F. Since the samples were stressed to give comparable strain rates, it follows that depletion in a given time at 1600°F was reduced. Despite this retarding influence, however, the amounts of depletion at fracture became comparable under influence of increased strain in Heats V + Zr, V + B, and V + B + Zr.

In samples ruptured at 1600°F and 25,000 psi (fig. 19) the depletion was extensive. Often, layers of precipitate-free matrix as thick as 5 to 10 microns were found. In this case, comparison of retardation was limited by the unequal exposure times and strains.

After 165 hours at 1600°F at an equal stress of 20,000 psi, the retarding effect of boron and zirconium was very evident. While 264 depleted boundaries were found in Heat V, only 72 were found in Heat V + Zr, 16 in Heat V + B and none in Heat V + B + Zr (table III).

Micro-cracks

Following agglomeration of $M_{23}C_6$ and depletion of γ' in the grain boundaries, micro-cracks appeared. These appeared as dark areas in mechanically polished samples (fig. 13). Confirming evidence of these was found in electron microscopy where the replicas contained fins

where the collodion had filled micro-cracks and then had been extracted during stripping of the replica from the metal surface. The fins appeared black in the electron microstructures (fig. 14) with white shadows from palladium.

The micro-cracks were associated with $M_{23}C_6$ particles in the grain boundaries transverse or nearly transverse to the applied stress, usually being at an $M_{23}C_6$ - matrix interface or between tips of $M_{23}C_6$ particles, in both cases where depletion of γ' had occurred. Often, several separate micro-cracks were detected in one grain boundary with no preference being shown for triple points. These separate cracks seemed to link together with further creep exposure; this constituting the mode of fracture in Heat V.

Figure 20 relates micro-cracking to creep deformation for the experimental heats exposed to give equal strain in equal time at 1600°F. Five micro-cracks were detected in Heat V at the end of first stage creep when only 15 percent of the rupture life was expended. The number of cracks for a given creep strain or exposure time diminished in Heat V + Zr, Heat V + B and Heat V + B + Zr in that order. In Heat V + B + Zr, only 2 micro-cracks were found at 80 percent of the rupture life when tertiary creep had already commenced. The amount of micro-cracking at fracture also diminished in the order Heat V, Heat V + Zr, Heat V + B and Heat V + B + Zr. When the four heats were exposed 165 hours at 1600°F and 20,000 psi, the difference in micro-cracking was even more pronounced. 314 micro-cracks were counted in Heat V, only 9 in Heat V + Zr and none in Heats V + B and V + B + Zr.

It was evident from the specimens tested at 1600°F and 25,000 psi that, although micro-cracking was retarded, it was not prevented by boron and zirconium (table III).

Intergranular Surface Cracking

In addition to micro-cracks within the specimens, the heats were subject to intergranular cracking from the specimen surface during creep-rupture tests. Initiation of these cracks was definitely from the specimen surface with a gradual increase in number and depth during creep exposure. Some of these cracks are pictured in figure 21 with quantitative data on amounts listed. Figure 21 shows that the specimen of Heat V run at 1600°F and 25,000 psi had negligible surface cracking at the time of rupture, 52 hours. The mode of fracture was by linking of the interior micro-cracks evident in figure 21. However, in Heat V + B run at 1600°F and 28,000 psi, the amount of micro-cracking was diminished but surface cracking is evident. The importance of these surface cracks in fracture is indicated by the sample from Heat V + B + Zr run at 1600°F and 30,000 psi, where some of the surface cracks penetrated more than 1/4 of the specimen radius.

The quantitative data for surface cracks seem to indicate that the trace element additions modified mode of fracture. Surface cracking increasingly competes with micro-cracking as a source of fracture when the tendency for micro-cracking is reduced.

Intragranular Precipitation of Carbide

In addition to decreased tendency for intergranular $M_{23}C_6$, a carbide precipitated intragranularly during exposure at 1600°F in the heats with boron more than in other heats (fig. 14).

The form of this phase was stress dependent. Short plate-like carbides formed in samples aged without stress. In the stress aged samples these were more elongated in form (compare figs. 13 and 17) and had a tendency to precipitate on preferred matrix planes. As

shown in figure 15, the phase was extracted from Heat V + B after 1.2 percent creep strain in 188 hours at 1600°F. The majority of spots in the electron diffraction pattern indexed for M_6C with some spots corresponding to $M_{23}C_6$. Therefore, it seemed that some of the intragranular carbide phase, if not all, was M_6C rather than $M_{23}C_6$.

The intragranular carbide was distributed fairly uniformly throughout the grains in the boron heats with some concentration near the Ti (C, N) particles.

There was some evidence that intragranular carbides diminished and carbides increased in the grain boundaries during long time exposure indicating that carbon was diffusing to the grain boundaries.

Intragranular γ'

The intragranular precipitates of γ' grew and agglomerated during aging at 1600°F. As measured by the surface density of γ' particles in electron micrographs there was no significant effect of boron, zirconium or stress on this reaction (fig. 22). Therefore, the differences in surface density of γ' existing after the 2150°F treatment and air cooling were not lasting and appeared to be unimportant.

As a further means of evaluating effects of trace elements on aging of γ' at 1600°F, the change of hardness with aging time at 1600°F was measured (fig. 23 and table IV). The hardness changes for the four experimental heats were very similar except that Heat V + B + Zr aged to a higher hardness and retained this advantage at 500 hours. All heats reached maximum hardness at 1600°F at about 1 hour and then overaged at longer times. Electron micrographs typical of the alloy showing γ' density are included in figure 23.

Although creep strain did not affect the density of γ' particles, it did modify the distribution of particles. Creep strains within the grains resulted in some preferential agglomeration of γ' on the slip planes, as evidenced by an alignment of γ'. This was especially noticeable after high creep strain (fig. 19).

Identification of the γ' phase was made by electron diffraction (fig. 15).

Nodular Precipitate

All the materials exhibited nodules to some extent after aging at 1600°F (fig. 24 and tables III and IV). The nodules, which often were seen to envelope or abut on carbon-rich Ti (C, N), appeared to be mixed carbide and γ'.

As shown in figure 24, their occurrence was definitely strain accelerated, especially in Heat V. Likewise, they were trace element controlled in that their formation was retarded by boron and zirconium.

Check of Boron Content after Creep Exposure

A specimen from Heat V + B was analyzed for boron content after rupture in 428 hours at 1600°F and 25,000 psi. The cross section of the specimen was analyzed at 0.0090 percent boron. A surface layer of approximately 0.010 inches depth contained 0.0079 percent boron. These compared with the analysis of 0.0089 percent boron obtained in the as-rolled bar stock.

DISCUSSION

The microstructural studies revealed the role of boron and zirconium in increasing creep-rupture life and ductility of the 55 Ni - 20 Cr - 15 Co - 4 Mo - 3 Ti - 3 Al alloy.

In the absence of boron and zirconium, $M_{23}C_6$ and γ' rapidly formed a network in the grain boundaries of the alloy during creep at 1600°F. This was followed by depletion of γ' precipitates in the metal adjacent to the transverse grain boundaries and early intergranular micro-cracking at the $M_{23}C_6$ - depleted zone interfaces. The micro-cracks grew, linked and initiated brittle and premature failure.

The role of boron and zirconium was to retard this grain boundary process, thereby allowing longer creep exposure and higher creep deformation before the fracture mechanism operated.

Additional experimental support for the mechanism is obtained by relating increasing creep-rupture life (fig. 25) and ductility (fig. 26) at 1600°F and 25,000 psi to the decreasing tendency of the experimental heats to undergo depletion of grain boundaries and micro-cracking during 1.2 percent creep deformation in 165 to 214 hours at 1600°F.

It is evident from the data that the increase in creep-rupture life and ductility from the trace element addition results from retardation, but not prevention, of the grain boundary mechanism of carbide formation, grain boundary depletion and micro-cracking. The specimens from all the experimental heats were similar in degree of grain boundary agglomeration of carbides, γ' depletion and micro-cracking after rupture at 1600°F and 25,000 psi. However, both the time and deformation at which the grain boundary effects occurred and initiated fracture were

increased by boron and zirconium.

The finding of only retardation of micro-cracking by boron and zirconium does not imply that their beneficial effects are only temporary in nickel base alloys. All available data indicate that the boron and zirconium materials are superior to those free of boron and zirconium even at low stresses and in long time exposure.

The chemical analyses on Heat V + B after rupture testing indicated that loss of boron from the sample during testing did not occur except possibly at the surface. De-boronization does not appear to be the cause of the eventual appearance of the grain boundary changes in boron bearing material.

Interpretation of Other Microstructural Changes

There are several other features of the data which require discussion.

Intragranular Carbide Precipitation

Apparently the occurrence of intragranular carbide in the heats with boron was related to retardation of $M_{23}C_6$ agglomeration in the grain boundaries. In a sense, a redistribution of carbide was affected by boron. In the case of zirconium additions, suppression of the grain boundary agglomeration was not accompanied by intragranular carbides, possibly because of the weaker effect at the grain boundary.

The intragranular carbide in the boron heats may have had a direct effect on properties in addition to tying up carbon to retard $M_{23}C_6$ agglomeration in grain boundaries. The form of the precipitate after creep indicates that it is strain induced and may lower creep rate

in a manner proposed by Cottrell[22]. According to Cottrell, resistance to creep is obtained by nucleation and growth of precipitates in dislocations, preventing further movement of the dislocations through the lattice. The reaction would resemble strain aging, although the resulting precipitate would be more advanced in growth than that usually associated with strain aging.

The negative creep and slight serrated effect in the creep curves of the boron heats at 1600°F and 20,000 psi appear to be additional evidence of strain induced precipitation. These phenomena have been observed in other nickel base alloys containing boron in unpublished work in this laboratory.

The presence of strain aging-type reactions in nickel base alloys is not totally unexpected in that Wache[23] has detected serrated stress-strain curves for 80 Ni - 20 Cr alloys up to 1292°F.

Although the above evidence indicates that strain induced carbide precipitate might have lowered creep rate, the proof was not considered positive.

Depletion

The depletion of γ' definitely required stress. No evidence of its occurrence was observed in any case when exposure was at 1600°F without stress. Furthermore, it was more prevalent in the transverse grain boundaries. The absence of γ' depletion when the alloy was aged at 1600°F without stress indicates that the reaction was not due to simple depletion of elements from the adjoining matrix by the grain boundary precipitates. It seems probable that the depletion mechanism was strain induced γ' agglomeration resulting from localized strain concentration at the grain boundaries.

Surface Cracking

The information obtained on the role of surface cracking was not sufficiently extensive to be sure of its role. The indications were that when boron or zirconium retarded micro-cracking to allow longer creep exposures or more highly stressed creep exposures, fracture was at least in part initiated by surface cracks.

Intragranular γ' Stability

It was thought initially that boron and zirconium might operate through some influence on the size, distribution or stability of the intragranular γ' reaction.

Since Baillie[11] succeeded in correlating creep-rupture properties with the surface density of γ' particles as measured in electron micrographs, surface density was used to detect possible effects of boron and zirconium on the γ' which would increase rupture life. No significant effect was found. In fact, these elements had so little effect on any aspect of γ' (other than in suppressing agglomeration and depletion of γ' at grain boundaries) that it seems certain that the boron-zirconium effect did not operate through the intragranular γ' reaction.

In the absence of any observable effect on the intragranular γ', the reason for the higher hardness of Heat V + B + Zr is uncertain. It was noted that the hardness values were in the same order as the total Ti + Al in the heats. The slightly higher Ti + Al may account for the higher hardness of Heat V + B + Zr.

The distribution of the γ' after creep exposure was found to be a good indicator of the mode and location of creep deformation. Alignment of γ' seemed to indicate that creep deformation had been accommodated by the grains as coarse slip. This alignment had previously been found

by Buckle and Poulignier to indicate the mode of deformation in nickel base alloys[24].

Nodular Precipitate

The role of the nodules of mixed carbide and γ' was not clear. No evidence was found to indicate that cracking was initiated by their presence. It is possible that nodules contributed to the depletion of γ' adjacent to the grain boundaries by acting as a final location for the γ'. This hypothesis is supported somewhat by the accelerating effect of stress on nodule formation at 1600°F, particularly when γ' depletion occurred.

Relation of Mechanism to Published Information

The accumulation of $M_{23}C_6$ in grain boundaries has striking parallels to sensitization of stainless steels. Simpkinson[25] and Bungardt and Lennartz[26] have identified $Cr_{23}C_6$ as the grain boundary phase leading to stress corrosion of 18-8 stainless steels. In addition, Plateau, Henry and Crussard[19] found the size, shape and distribution of $Cr_{23}C_6$ in 18-8 stainless steels to be similar to that of $M_{23}C_6$ found in this study.

The agglomeration at grain boundaries during creep of Ti + Al hardened nickel base alloys has been noted by Baillie and Poulignier[15] and Mathieu[16]. The γ' and $M_{23}C_6$ network could influence properties in two ways. The $M_{23}C_6$ particles could act as heterogeneous nuclei for micro-cracks, lowering the requirements for micro-cracking. Also a continuous film in the grain boundaries can lead to stress concentrations at the grain boundaries. Strain on the slip planes running up to the grain

boundary from one grain cannot pass into the adjoining grain because of blocking by the film[27]. Thus, the opportunity for stress relief is reduced.

In accordance with the theories of Chang and Grant[27], depletion of precipitates in layers of matrix adjacent to grain boundaries would promote micro-cracking and fracture by concentrating deformation at these weak grain boundaries. It is possible that this mechanism operates in many high temperature alloys to give brittle fractures when the creep resistance of the material remains high. Such an explanation was offered by Wever and Schrader[28] for brittle fracture of Cr - Ni - Mo steels in long time service at 500°C. Localized precipitation of Mo_2C left a condition of strong grains and depleted grain boundaries. Further confirmation is obtained from work on the effect of cellular precipitation[29,30] where this left depleted regions in the grain boundaries and led to premature and brittle creep-rupture.

The limited success met in the literature in correlating creep-rupture properties with intragranular γ' dispersion is at least partially explained by the results. When the Ti + Al hardened nickel base alloys are exposed at temperatures low in the aging range for γ', the tendency for agglomeration and overaging at grain boundaries is low and creep tends to be intragranular and dependent on the dispersion of intragranular precipitates. However, creep exposure high in the aging range for γ' leads to agglomeration, overaging and severe weakening at grain boundaries. In this condition, the creep-rupture properties are limited by the grain boundary conditions and are not as much a function of the intragranular γ' dispersion.

The location of micro-cracks at the $M_{23}C_6$ - matrix interface was

interesting in light of the work of Resnick and Seigle[31], who established that ZnO particles were heterogeneous nuclei for micro-cracks in α-brass. As shown by Machlin[32], particle - matrix bonding is important in nucleation of micro-cracks. In general, the presence of second phase particles makes nucleation more probable, especially when bonding is poor. Considering these effects, it seems probable that the $M_{23}C_6$ particles acted as nuclei for micro-cracks; possibly because of poor bonding.

The mechanism of nucleation and growth of micro-cracks is not clear. Several authors[31,32,33,34,35] have proposed condensation of vacancies formed during creep by dislocation movements. Others[27,36,37] emphasized that local stress concentrations were the cause. Grain boundary sliding is usually considered to set up the local stress concentrations at the transverse boundaries to cause loss of cohesion. Chang and Grant[27] hypothesized that rate of growth of micro-cracks in grain boundaries depends upon the stress pattern at the boundaries. Propagation of micro-cracking is caused primarily by the normal stress at the grain boundary and the inability of the material to relieve this stress. The overall rate of growth depends upon the ability of the grains to accommodate the normal stresses by deformation within the grain. From this it can be inferred that micro-cracking increases as the severity of localization of deformation at grain boundaries increases. Therefore, change of the mode of deformation from intragranular slip to grain boundary creep can be expected to increase grain boundary micro-cracking by redistribution of stresses. In fact, in α-brass the occurrence of micro-cracking is coincident with the change from coarse slip to grain boundary sliding[33]. The evidence of increased intragranular slip and decreased micro-cracking in the boron and

zirconium heats is in full agreement with the above theories. It appears feasible that the elements have changed the mode of deformation by maintaining the grain boundary strength.

The discrepancies of the literature on the time of micro-crack nucleation are not surprising, considering the effect of trace elements in this study. While several instances have been found of micro-cracking early in second stage creep[34,38,39], other cases exist where none was found until tertiary creep[33,40,41]. In this study, the case exists where, in one alloy, nucleation of micro-cracks can be delayed from early in second stage to early in third stage creep by trace elements.

Regarding the effect of micro-cracks on properties, the Russian theorists[35,39,42] attribute tertiary creep and rupture to a gradual destruction of the metal by micro-cracking. This implies that micro-cracking raises creep rate and lowers life and ductility. In addition, the normal break in the stress-rupture curve of commercial alloys associated with a change from transgranular to intergranular fracture is an important consideration. This change in fracture mechanism, which is essentially an increase in intergranular micro-cracking, results in lower life and ductility than predicted from higher stress data where micro-cracking was less predominant.

In general, the literature supports the mechanism established. The grain boundary process would be expected to raise creep rate and lower rupture life and ductility. It follows that retardation of the grain boundary changes by boron and zirconium would be the mechanism for the beneficial effects on properties.

Causes of Effect of Boron and Zirconium on Grain Boundary Stability

The experimental evidence established that trace amounts of boron

and zirconium retard agglomeration at grain boundaries and thereby retard the micro-cracking mechanism. Several causes of this retardation of agglomeration might be proposed.

It can be hypothesized that boron and zirconium stabilize carbon directly in a less deliterious form than intergranular $M_{23}C_6$ in the same manner that titanium stabilizes carbon as Ti C in 18-8 stainless steels. One would expect to find evidence of boron-carbon or zirconium-carbon compounds in this case. Since none were detected, support for this theory is lacking.

A similar possibility would be that the elements are promoting stabilization of carbon indirectly by promoting the nucleation and growth of one carbide at the expense of another. This might result from solid solution of boron or zirconium in the complex carbides of the M_6C or $M_{23}C_6$ type. Indeed, the detection of intragranular carbides, apparently of the M_6C type, when boron was present is compatible with this hypothesis. However, lack of promotion of additional carbides by zirconium additions does not support this hypothesis.

An alternative reason might be found in equilibrium segregation. Cahn[43] has reviewed the relationships of grain boundaries to impurity distribution. When elements of odd atomic size exist in alloys, they are subject to inhomogeneous distribution. Because they do not fit well in the crystal lattice where high regularity exists, the odd sized atoms segregate to regions of lower regularity where larger vacancies exist. Grain boundaries are a prime region of concentration because of their inherent irregularity. Experimental confirmation for this was obtained by Thomas and Chalmers[44] who found that polonium segregates to grain boundaries in Pb - Bi alloys.

The segregating tendencies of two competing odd sized elements can be related to their degree of misfit in that the most odd sized atoms will seek out the grain boundary more rapidly. Thus, small amounts of one very odd sized element can be utilized to heal the grain boundary, thereby retarding the segregation of a less odd sized element by decreasing the available holes and energy of the grain boundary. The possibility exists that boron and zirconium are retarding carbon segregation by this mechanism.

Study of the atomic diameters of carbon, boron and zirconium might reveal the feasibility of this. Speiser, Spretnak and Taylor[45] have shown that the effective diameter of carbon in γ-Fe is 1.36 Å, while they postulate that boron has an effective diameter equivalent to or greater than 1.85 - 1.90 Å. Goldschmidt's metallic diameter (for coordination number of 12) for zirconium is 3.20 Å. The available lattice spaces in the 55 Ni - 20 Cr - 15 Co - 4 Mo - 3 Ti - 3 Al alloy can be calculated from the lattice parameter of 3.58 Å established in unpublished work at this laboratory. The vacant interstitial space in solid solution is 1.05 Å in diameter. Using the data on atomic diameters, the carbon atom is 29 percent larger, boron is 78 percent larger and zirconium is 200 percent larger than the available space. In the case of substitutional solution, the boron atom is 26 percent smaller, and zirconium 27 percent larger than the substitutional space of 2.52 Å diameter. Therefore, it appears that carbon fits moderately well interstitially but that boron and zirconium fit poorly both as interstitials and in substitution. Then it seems feasible that boron and zirconium are segregating preferentially to grain boundaries, healing them and retarding carbon segregation.

Other aspects of the data lend support to the theory of equilibrium segregation. Decreased tendency for γ' agglomeration at the grain boundaries in the boron and zirconium heats could result from the boron and zirconium healing the grain boundaries. The promotion of intragranular carbide by boron might be the indirect result of this. The decreased segregation would leave a higher carbon content within the grains, making precipitation of intragranular carbides more probable.

Additional support for the theory of equilibrium segregation is in the literature. Brown[46] proposed that boron additions beneficiated iron base alloys by this mechanism. Strauss[47] emphasized that marked beneficiation of properties by trace element additions usually occurs with elements with characteristics which would lead to segregation to grain boundaries.

Role of Carbon

The apparent harmful effect of $M_{23}C_6$ in the grain boundaries of the alloy and the possible helpful effect of the intragranular carbide promoted by boron make the role of carbon in nickel base alloys of great interest.

One might conclude from the results that the relatively carbon-free alloy would be free of the grain boundary carbide agglomeration and, therefore, have properties equivalent to Heat V + B + Zr. This, however, is not the case. It has been shown in unpublished work at this laboratory that both rupture life and ductility increase as carbon is increased from less than 0.01 to 0.04 percent in the boron and zirconium-free alloy. Therefore, it seems that carbon can also have

a beneficial role in the alloy. The reason for this effect is not at all clear at this time but it could be one of several mechanisms including improved degassing, solid solution strengthening or prevention of other embrittling grain boundary reactions.

Generality of Results

It is expected that boron and zirconium generally will be found to suppress the agglomeration of phases in grain boundaries and subsequent micro-cracking in complex heat resistant alloys during creep. While this mechanism should be generally applicable, the details of the effects can be expected to vary with several factors.

Within a specific alloy, there should be variations depending on hot working and heat treating history. This would probably result from differences in cold work, grain size and amount and distribution of phases before creep exposure. Modification can be expected with varying test conditions. The mechanism of creep can be expected to vary with test temperature and stress. Conditions which favor creep within the grains (temperatures on the low side of the creep range and high stresses) should reduce the effectiveness of boron and zirconium under the mechanism observed.

In addition, variations can be expected with changes in major precipitation hardening elements. Since a portion of the agglomerated network was γ', it can be expected that the severity of agglomeration (and the magnitude of retardation by boron and zirconium) will be proportional to Ti + Al content. It is probable that alloys designed to yield beneficial age hardening reactions other than γ' would have tendencies for localized precipitation and agglomeration of the hardening

phase at grain boundaries. This tendency should be counteracted by the trace elements.

Changes in the content of alloying elements participating in carbide reactions should modify the carbide transformations and the effectiveness of the trace elements. An example is found in comparing the magnitude of the boron effect in Waspaloy and M252 alloys[2]. The less pronounced benefit of boron in M252 alloy is apparently related to a higher molybdenum content which favors innocuous M_6C - type carbides rather than the deliterious $M_{23}C_6$ - type carbide networks in grain boundaries. Since the tendency for the carbide network is lower than in Waspaloy alloy, the retarding effect of boron is less evident as property effects. Addition of strong carbide stabilizers such as columbium would tie up carbon to diminish the amount of grain boundary $M_{23}C_6$, thereby decreasing the need for trace elements.

The data suggest that the pronounced effects of harmful trace elements (Pb, S) and other helpful ones (Mg) also may arise from equilibrium segregation to grain boundaries. In addition, the complex interaction effects of trace elements in nickel base alloys may arise from competition in segregation and not from formation of compounds by the interacting elements. It is believed that a broad fundamental study of equilibrium segregation of many beneficial and detrimental trace elements alone and in combination in nickel base alloys would be a significant contribution to the literature.

There are implications of the data about alloy design for high temperature service. First, the importance of proper "stabilization" of carbon is apparent. Secondly, the required balance between intragranular and intergranular creep resistance is apparent. Not only is

it important to design alloys for high intragranular creep resistance by such devices as finely dispersed age hardening phases or mechanical dispersions; but also, it is necessary to maintain the strength of grain boundaries to prevent concentration of creep at grain boundaries. Therefore, alloy design becomes a complex pattern of adjusting intragranular hardeners such as Ti + Al with proper amounts of grain boundary stabilizers such as boron and zirconium.

CONCLUSIONS

Trace amounts of boron and zirconium increase creep-rupture properties of the complex Ti + Al hardened nickel base alloy by retarding structural changes at the grain boundaries. In the absence of these elements, $M_{23}C_6$ and γ' agglomerate rapidly in the grain boundaries. Subsequently, the matrix material adjacent to the grain boundaries transverse to the applied stress becomes depleted of γ' precipitates. Micro-cracks then develop at the $M_{23}C_6$ - depleted matrix interfaces, grow and combine to initiate brittle and premature fracture.

Zirconium, boron and boron plus zirconium in the proper amounts retard these changes, with effectiveness increasing in the order listed, to allow longer life to higher deformations before fracture occurs. While micro-cracking was detected early in second stage creep at relatively short time periods in the absence of boron and zirconium, proper amounts of boron and zirconium delayed micro-cracking until after third stage creep started after long creep exposure.

Creep-rupture properties at 1600°F of the material correlated with the stability of the grain boundaries. The property effects were not found to result from a change in the size, amount and distribution of the general intragranular γ'.

Some possible causes of the stabilizing influence of boron and zirconium on the grain boundaries have been discussed. Of these, retardation of agglomeration by preferential segregation of boron and zirconium to grain boundaries fits the data best.

REFERENCES

1. Decker, R. F., Rowe, J. P., Freeman, J. W. : "Influence of Crucible Materials on High-Temperature Properties of Vacuum-Melted Nickel - Chromium - Cobalt Alloy." NACA TN 4049, 1957.

2. Koffler, R. W., Pennington, W. J., Richmond, F. M. : "The Effect of Small Amounts of Boron and Zirconium on the High Temperature Properties of Vacuum-Melted Super Alloys." Report 48, Research and Development Department, Universal-Cyclops Steel Corporation, Bridgeville, Pa., June 11, 1956.

3. Darmara, F. N. : "Quality Control Achieved by Vacuum Melting and Effects on High Temperature Properties." Paper presented at Regional High-Temperature Materials Conference of Cleveland Section of AIME, April 17, 1957.

4. Jones, W. E. : "Vacuum Induction Melting-Process Considerations." Metal Progress, Vol. 72, Oct. 1957, p. 133.

5. Nordheim, R., Grant, N. J. : "Aging Characteristics of Nickel-Chromium Alloys Hardened with Titanium and Aluminum." Journal of Metals, Vol. 6, 1954, p. 211.

6. Taylor, A. : "Constitution of Nickel-Rich Quaternary Alloys of the Ni - Cr - Ti - Al System." Journal of Metals, Vol. 8, 1956, p. 1356.

7. Betteridge, W., Franklin, A. W. : "Progress in Nickel-Chromium Base Alloys for Service at High Temperatures." Revue de Métallurgie, Vol. 53, 1956, p. 271. (French).

8. Frey, D. N., Freeman, J. W., White, A. E. : "Fundamental Aging Effects Influencing High-Temperature Properties of Solution Treated Inconel X." NACA TN 2385, 1951.

9. Brockway, L. O., Bigelow, W. C. : "The Investigation of the Minor Phases of Heat-Resistant Alloys by Electron Diffraction and Electron Microscopy," WADC TR 54-589, Wright-Patterson Air Force Base, Ohio, May 1955.

10. Betteridge, W., Smith, R. A. : "Effect of Heat Treatment and Structure Upon Creep Properties of Nimonic Alloys Between 750° and 950°C." Symposium on Metallic Materials for Service at Temperatures above 1600°F. ASTM, 1956, p. 29.

11. Baillie, Y. : "Some Results of an Electron Microscopic Study of Ni - Cr - Al - Ti Alloys Used in Aircraft Turbines." Revue Universelles des Mines, Vol. 12, 1956, p. 507. (French).

12. Beattie, H. J., VerSnyder, F. L. : "The Influence of Molybdenum on the Phase Relationships of a High Temperature Alloy." Trans. ASM, Vol. 49, 1957, p. 883.

13. Wilde, R. F., Grant, N. J. : "Aging in Complex Commercial Ni - Cr Alloys Hardened with Titanium and Aluminum." Journal of Metals, Vol. 9, 1957, p. 865.

14. Betteridge, W., Franklin, A. W. : "The Effect of Heat-Treatment and Structure on The Creep and Stress-Rupture Properties of Nimonic 80A." The Journal of the Institute of Metals, Vol. 85, 1957, p. 473.

15. Baillie, Y., Poulignier, J. : "Submicroscopic Precipitation in Heat-Resistant Nickel-Chromium Alloys." Revue de Métallurgie, Vol. 51, 1954, p. 179. (French).

16. Mathieu, M. : "Contribution to the Knowledge of Modified Heat-Resistant 80 Ni - 20 Cr Alloys." La Recherche Aeronautique, Vol. 51, May-June 1956, p. 43. (French).

17. Bigelow, W. C., Amy, J. A., Brockway, L. O. : "Electron Microscopic Identification of the γ' Phase of Nickel-Base Alloys." Proc. ASTM, Vol. 56, 1956, p. 945.

18. Fisher, R. M. : "Electron Microstructure of Steels by Extraction Replica Technique." Symposium on Techniques for Electron Metallography, ASTM, 1953, p. 49.

19. Plateau, J., Henry, G., Crussard, C. : "Some New Applications of Microfractography." Revue de Metallurgie, Vol. 54, 1957, p. 200. (French).

20. Bradley, D. E. : "Evaporated Carbon Films for Use in Electron Microscopy." British Journal of Applied Physics, Vol. 5, 1954, p. 65.

21. Fullam, E. F. : "Replica Washing Methods." Symposium on Techniques for Electron Metallography, ASTM, 1953, p. 101.

22. Cottrell, A. H. : "Creep and Aging Effects in Solid Solutions." Creep and Fracture of Metals at High Temperatures. Her Majesty's Stationery Office, London, 1956, p. 141.

23. Wache, X. : "Discontinuous Elongation of Austenitic - 80 Nickel, 20 Chromium Alloy and Elinvar Subjected to an Ordinary Tensile Test at High Temperature." Comptes Rendus, Vol. 240, 1955, p. 1892. (French).

24. Buckle, Ch., Poulignier, J. : "A Metallographic Study of Cold Working on Heat Resisting 80-20 Nickel-Chromium Alloys." Revue de Métallurgie, Vol. 53, March 1956, p. 179. (French).

25. Simpkinson, T. V. : "Metallography of Titanium-Stabilized 18-8 Stainless Steels." Trans. ASM, Vol. 39, 1947, p. 721.

26. Bungardt, K., Lennartz, G. : Archiv Für Das Eisenhüttenwesen, Vol. 27, 1956, p. 127. (German).

27. Chang, H. C., Grant, N. J. : "Mechanism of Intercrystalline Fracture," Journal of Metals, Vol. 8, 1956, p. 544.

28. Wever, F., Schrader, H. : "Electron Microscopy of Changes in Structure of Cr - Ni - Mo Steel Under Long-Time Tension Stress at 500°C." Archiv Für Das Eisenhüttenwesen, Vol. 26, 1955, p. 475. (German).

29. Roberts, C. S. : "Interaction of Precipitation and Creep in Mg - Al Alloys." Journal of Metals, Vol. 8, 1956, p. 146.

30. Sully, A. H. : Discussion in Creep and Fracture of Metals at High Temperatures. Her Majesty's Stationery Office, London, 1956, p. 308.

31. Resnick, R., Seigle, L. : "Nucleation of Voids in Metals During Diffusion and Creep." Journal of Metals, Vol. 9, 1957, p. 87.

32. Machlin, E. S.: "Creep-Rupture by Vacancy Condensation." Journal of Metals, Vol. 8, 1956, p. 106.

33. Greenwood, J. N., Miller, D. R., Suiter, J. W. : "Intergranular Cavitation in Stressed Metals." Acta Metallurgica, Vol. 2, 1954, p. 250.

34. Crussard, C., Friedel, J. : "Theory of Accelerated Creep and Rupture." Creep and Fracture of Metals at High Temperatures. Her Majesty's Stationery Office, London, 1956, p. 243.

35. Guy, A. G. : "Russian Theory for Creep Fracture." Metal Progress, Vol. 69, March 1956, p. 158.

36. McLean, D. : "A Note on the Metallography of Cracking During Creep." The Journal of the Institute of Metals, Vol. 85, 1957, p. 468.

37. Nield, B. J., Quarrell, A. G. : "Intercrystalline Cracking in Creep of Some Aluminum Alloys." The Journal of the Institute of Metals, Vol. 85, 1957, p. 480.

38. Nield, B. J. : "Discussion in Creep and Fracture of Metals at High Temperatures. Her Majesty's Stationery Office, London, 1956, p. 308.

39. Kishkin, S. T. : "Mechanism of Weakening and Fracture of Crystalline Bodies as a Function of Time at High Temperature." Doklady Akademii Nauk SSSR, Vol. 95, 1954, p. 789. (Russian).

40. McAdam, D. J., Giel, G. W., Woodard, D. H. : "Influence of Strain Rate and Temperature on the Mechanical Properties of Monel Metal and Copper." Proc. ASTM, Vol. 46, 1946, p. 902.

41. Kirkby, H. W. : Discussion in Creep and Fracture of Metals at High Temperatures. Her Majesty's Stationery Office, London, 1956, p. 331.

42. Dekhtiar, I. I., Osipov, K. A. : "Fracture of Metals at High Temperatures." Doklady Akademii Nauk SSSR, Vol. 104, 1955, p. 229. (Russian).

43. Cahn, R. W. : "Grain Boundaries, Substructures and Impurities." Impurities and Imperfections. ASM, 1955, p. 41.

44. Thomas, W. R., Chalmers, B. : "The Segregation of Impurities to Grain Boundaries." Acta Metallurgica, Vol. 3, Jan. 1955, p. 17.

45. Speiser, R., Spretnak J. W., Taylor, W. J. : "Effective Diameter of Solute Atoms in Interstitial Solid Solution." Trans. ASM, Vol. 46, 1954, p. 1168.

46. Brown, J. T., Bulina, J. : "W-545 - A New High Temperature Turbine Disc Alloy." Paper presented at Regional High-Temperature Materials Conference of Cleveland Section of AIME, April 16, 1957.

47. Strauss, J. : "Micrometallurgy - The Metallurgy of Minute Additions." Proc. ASTM, Vol. 53, 1953, p. 577.

TABLE I

Chemical Analyses of Experimental Heats

(weight percent as rolled)

Heat	B	Zr	Cr	Co	Mo	Ti	Al	Si	Mn	C	S	P	Mg	Fe	Cu
V	.0002	<.01	19.7	15.0	3.90	3.08	3.35	.17	.13	.08	.007	.006	<.01	<.30	<.10
V + Zr	.0004	.19	18.8	15.1	4.15	3.14	3.14	.10	<.10	.08	.008	.003	--	<.30	--
V + B	.0089 .0090[1] .0079[2]	<.01	20.9	14.8	4.20	3.15	3.25	.20	<.10	.10	--	.004	<.01	<.30	<.10
V + B + Zr	.0088	.01	20.8	14.8	4.20	3.20	3.30	.19	.11	.09	--	.007	<.01	<.30	<.10

1. Analysis on cross section of 0.250-inch diameter rupture specimen after 428 hours at 1600°F.

2. Analysis on 0.010-inch surface layer of sample described in 1.

TABLE II

Creep-Rupture Data at 1600°F

(Initial Condition - 2 hours at 2150°F, air cooled + 4 hours preheat at 1600°F before loading)

Heat	Stress (psi)	Minimum Second Stage Creep Rate (%/hr)	Rupture			Interruption	
			Time (hr)	Elongation (%)	Reduction of Area (%)	Time (hr)	Total Deformation (%)
V	25,000	0.0160	45	2	1	--	--
	25,000	0.0060	52	2	1	--	--
	20,000	0.0070	158	3	2	--	--
	20,000	0.0040	--	--	--	165	1.23
	20,000	0.0058	--	--	--	117	1.00
	20,000	0.0046	--	--	--	85	0.76
	20,000	0.0052	--	--	--	85	0.76
	20,000	0.0084	--	--	--	47	0.55
	20,000	0.0058	--	--	--	23	0.29
V + Zr	25,000	0.0036	147	5	5	--	--
	25,000	0.0095	134	6	8	--	--
	22,500	0.0032	208	5	4	--	--
	22,500	0.0036	--	--	--	172	1.25
	20,000	0.0027	--	--	--	165	0.63
V + B	28,000	0.0025	296	10	14	--	--
	28,000	0.0040	--	--	--	214	3.45
	28,000	--	--	--	--	188	1.21
	28,000	0.0046	--	--	--	68	0.56
	25,000	0.0018	429	10	11	--	--
	25,000	--	394	7	8	--	--
	20,000	negative	--	--	--	165	0.15
V + B + Zr	30,000	0.0021	266	8	9	--	--
	30,000	--	--	--	--	214	1.18
	25,000	0.0004	666	17	16	--	--
	25,000	0.0003	627	12	13	--	--
	20,000	negative	--	--	--	165	0.04

TABLE III

Properties of Specimens Stress Aged at 1600°F

Condition	Heat V				Heat V + Zr				Heat V + B				Heat V + B + Zr			
	Nodules[1]	γ' density[2]	Depleted Grain Boundaries	Micro-cracks	Nodules	γ' density	Depleted Grain Boundaries	Micro-cracks	Nodules	γ' density	Depleted Grain Boundaries	Micro-cracks[4]	Nodules	γ' density	Depleted Grain Boundaries	Micro-cracks
Equal Strain Rate Study																
0.3% creep deformation	239	--	49	5	--	--	--	--	--	--	--	--	--	--	--	--
0.6% creep deformation	301	--	76	17	--	--	--	--	5	--	2	2	--	--	--	--
0.8% creep deformation	332	--	184	34	--	--	--	--	--	--	--	--	--	--	--	--
	288	--	173	31	--	--	--	--	--	--	--	--	--	--	--	--
1.0% creep deformation	334	--	151	118	--	--	--	--	--	--	--	--	--	--	--	--
1.2% creep deformation	418	134	264	314	175	137	127	78	63	157	60	30	20	117	23	2
3.5% creep deformation	--	--	--	--	--	--	--	--	79	--	165	77	--	--	--	--
ruptured	532	--	764	958	228	--	568	532	176	--	676	243	86	--	538	198
Equal Stress Study																
165 hours at 20,000 psi	418	134	264	314	129	151	72	9	25	158	16	none detected	0	125	none detected	none detected
ruptured at 25,000 psi	225	256	192	374	254	109	916	145	145	67	442	166	86	51	661	402
	218	--	211	378	--	--	--	--	--	--	--	--	90	--	530	330

1. Mixed carbide and γ' nodule greater than 5 microns diameter, number in 0.008 square inches.

2. γ' particles per square inch at 12,000D.

3. Grain boundaries where depletion was detected at 1000D, number in 0.008 square inches.

4. Micro-cracks detected at 1000D, number in 0.008 square inches.

TABLE IV

Properties of Specimens Aged at 1600°F Without Stress

Aging Time (hr)	Heat V			Heat V + Zr			Heat V + B			Heat V + B + Zr		
	DPH	Nodules[1]	γ' density[2]	DPH	Nodules	γ' density	DPH	Nodules	γ' density	DPH	Nodules	γ' density
0.5	359	--	--	354	--	--	357	--	--	373	--	--
1	364	--	--	362	--	--	362	--	--	380	--	--
4	359	--	--	353	--	--	357	--	--	366	--	--
10	355	45	588	348	32	544	348	16	768	362	0	584
100	345	180	134	346	57	147	346	33	168	355	19	137
188	338	--	107	342	--	116	340	--	101	353	--	103
500	335	300	65	344	139	67	339	149	68	344	25	64

1 Nodules greater than 5 microns diameter, number in 0.008 square inches.

2 γ' particles per square inch at 12,000D.

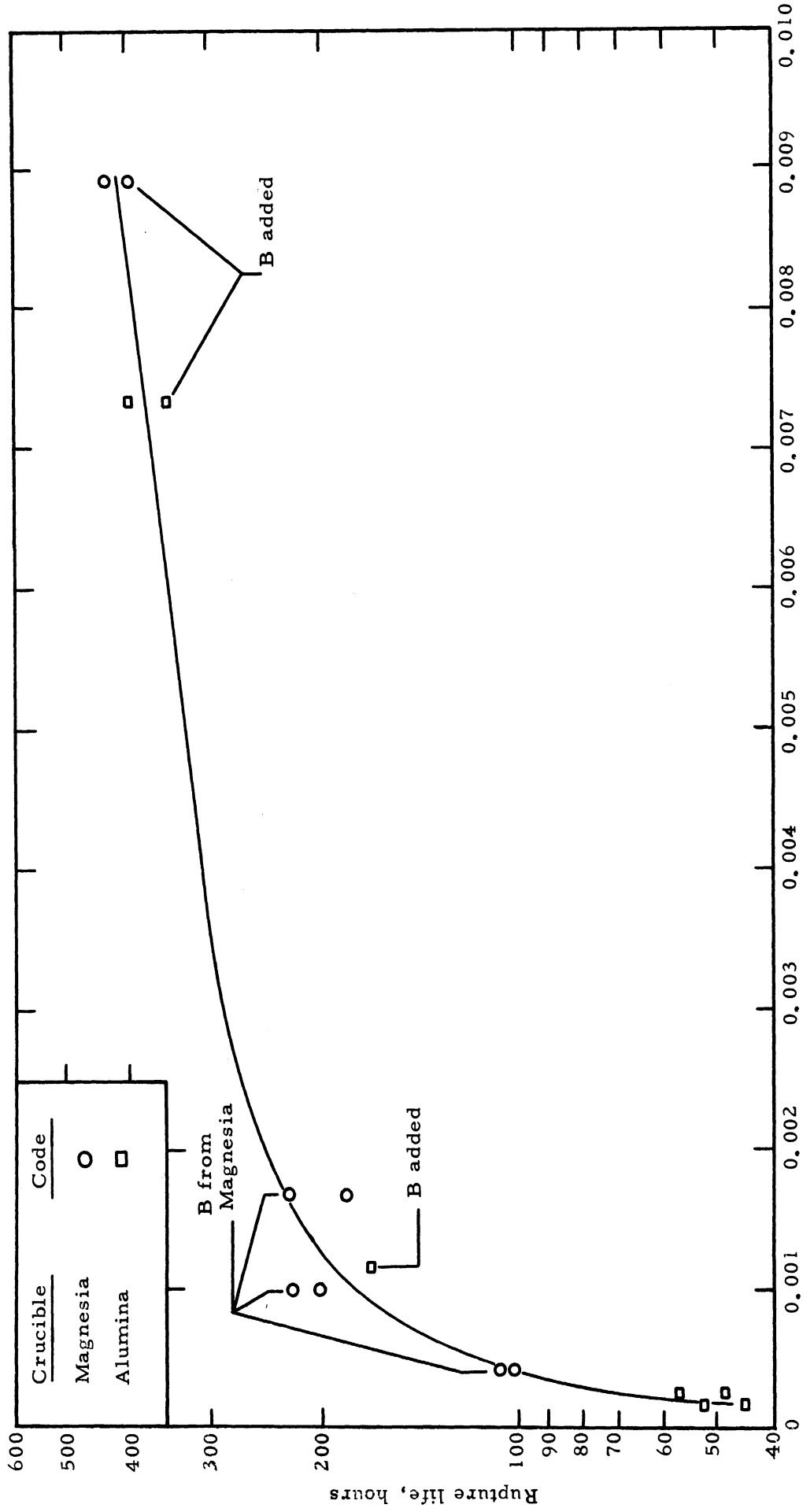

Figure 1. - Effect of boron content on rupture life at 1600°F and 25,000 psi of experimental heats of 55 Ni - 20 Cr - 15 Co - 4 Mo - 3 Ti - 3 Al alloy (with less than 0.01% Zr). Heat treatment prior to testing was 2 hours at 2150°F, air cooled plus 4 hours preheat at 1600°F. Decker, Rowe and Freeman [1].

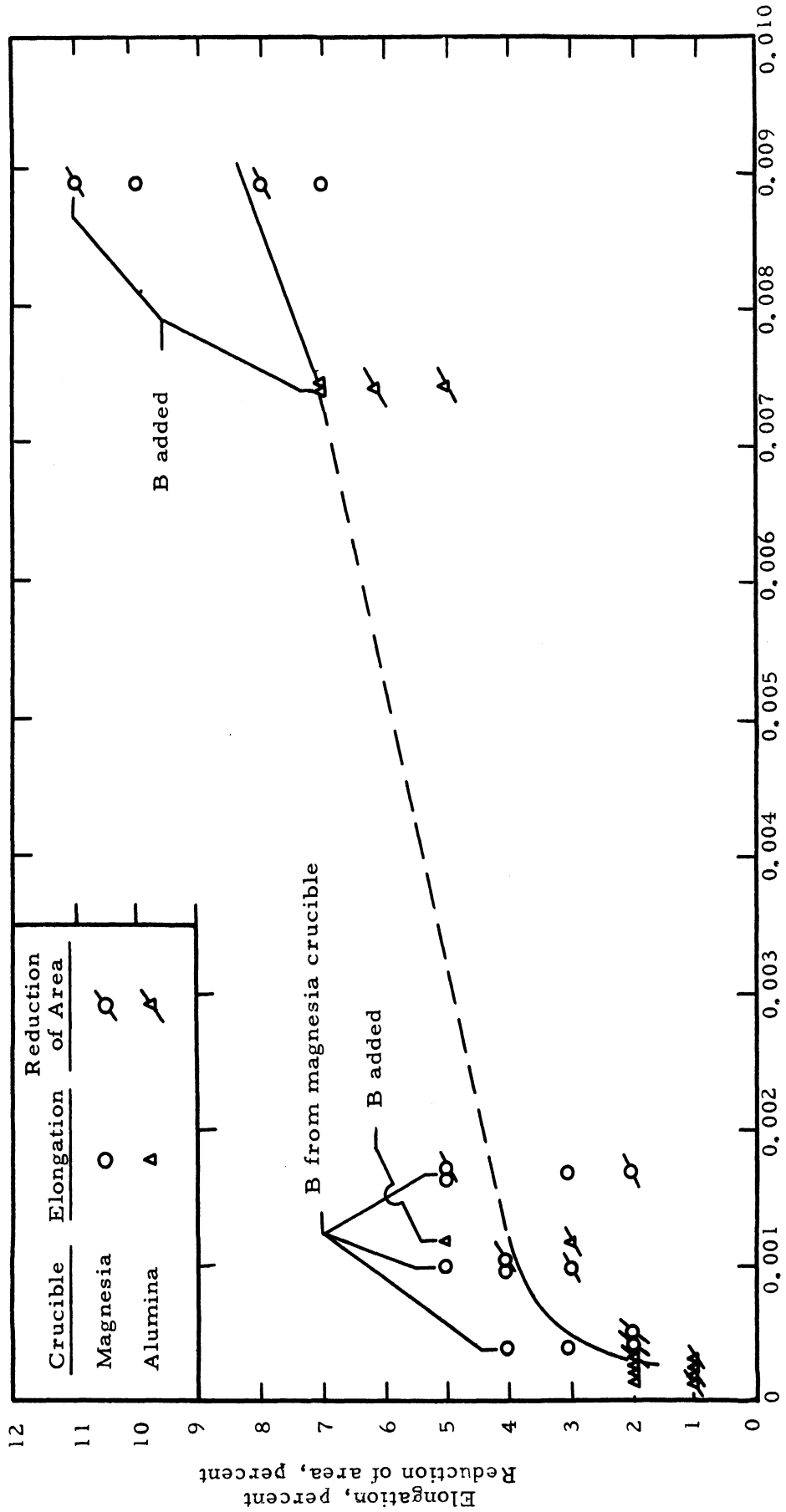

Figure 2. - Effect of boron content on ductility at 1600°F and 25,000 psi of experimental heats of 55 Ni - 20 Cr - 15 Co - 4 Mo - 3 Ti - 3 Al alloy (with less than 0.01% Zr). Heat treatment prior to testing was 2 hours at 2150°F, air cooled plus 4 hours preheat at 1600°F. Decker, Rowe and Freeman [1].

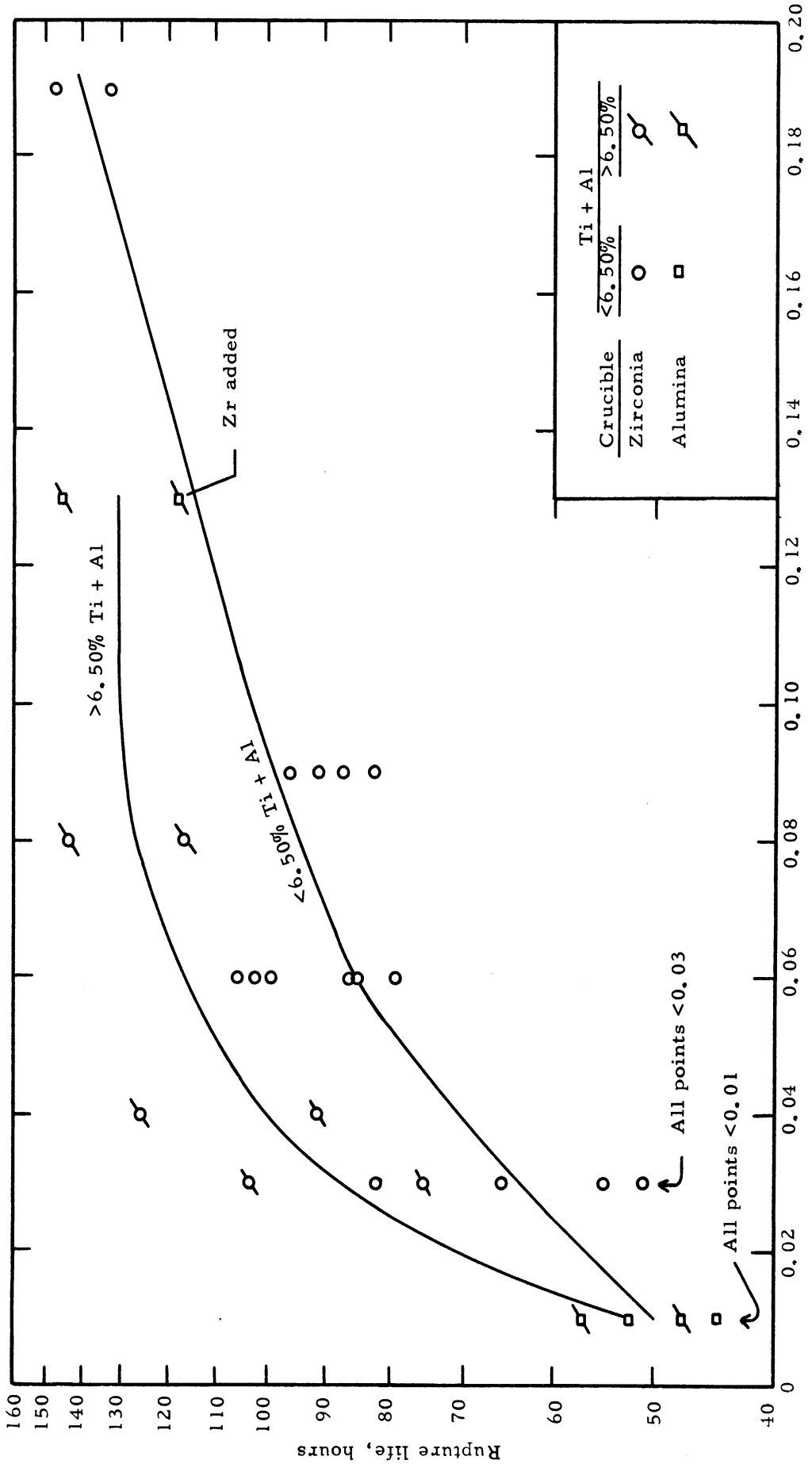

Figure 3. - Effect of zirconium content on rupture life at 1600°F and 25,000 psi of experimental 55 Ni - 20 Cr - 15 Co - 4 Mo - 3 Ti - 3 Al alloy (with less than 0.0005% B). Heat treatment prior to testing was 2 hours at 2150°F, air cooled plus 4 hours preheat at 1600°F. Decker, Rowe and Freeman [1].

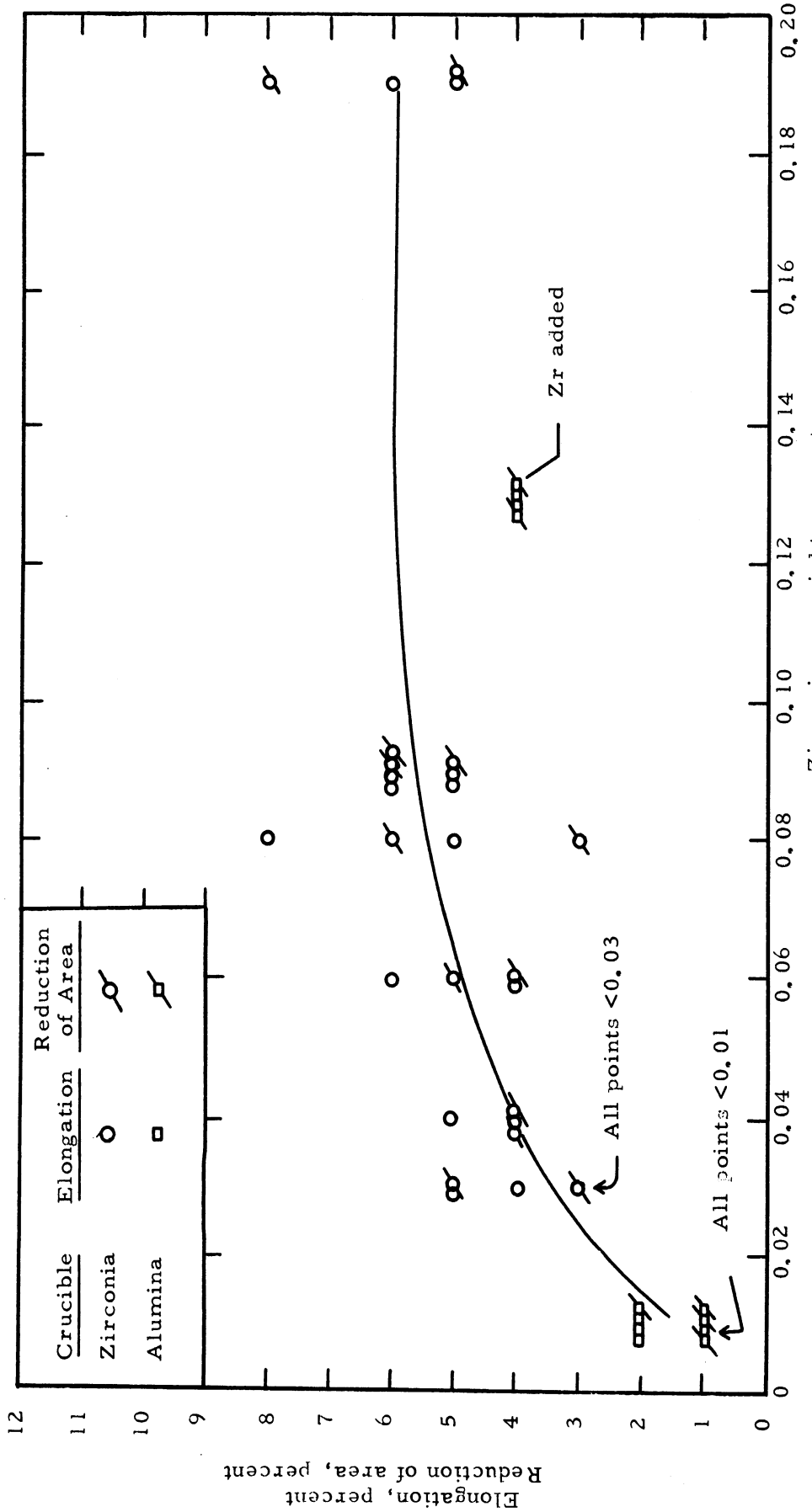

Figure 4. - Effect of zirconium content on ductility at 1600°F and 25,000 psi of experimental heats of 55 Ni - 20 Cr - 15 Co - 4 Mo - 3 Ti - 3 Al alloy (with less than 0.0005% B and between 0.04 to 0.09% C). Heat treatment prior to testing was 2 hours at 2150°F, air cooled plus 4 hours preheat at 1600°F. Decker, Rowe and Freeman [1].

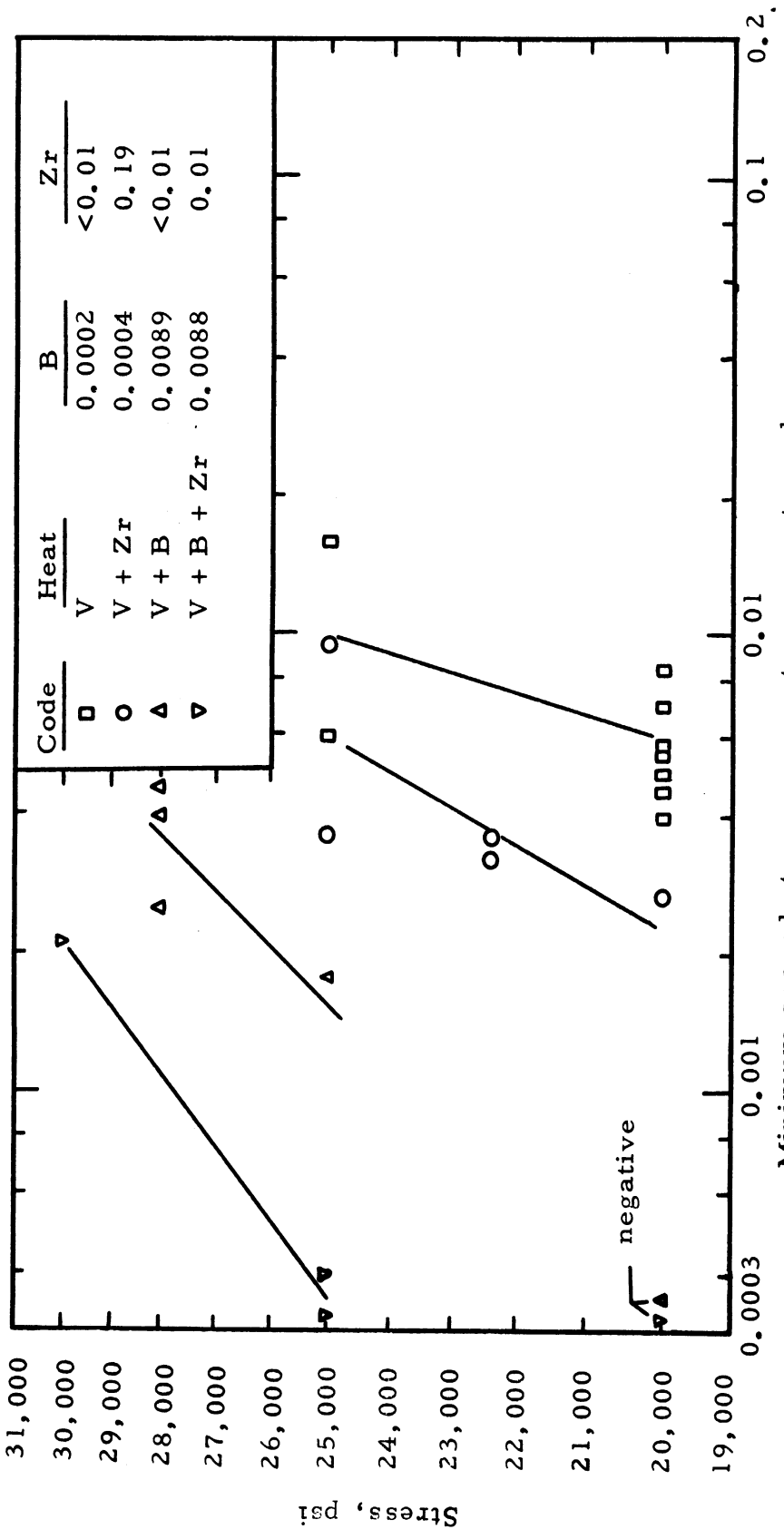

Figure 5. - Influence of stress on minimum second stage creep rate at 1600°F for the experimental heats.

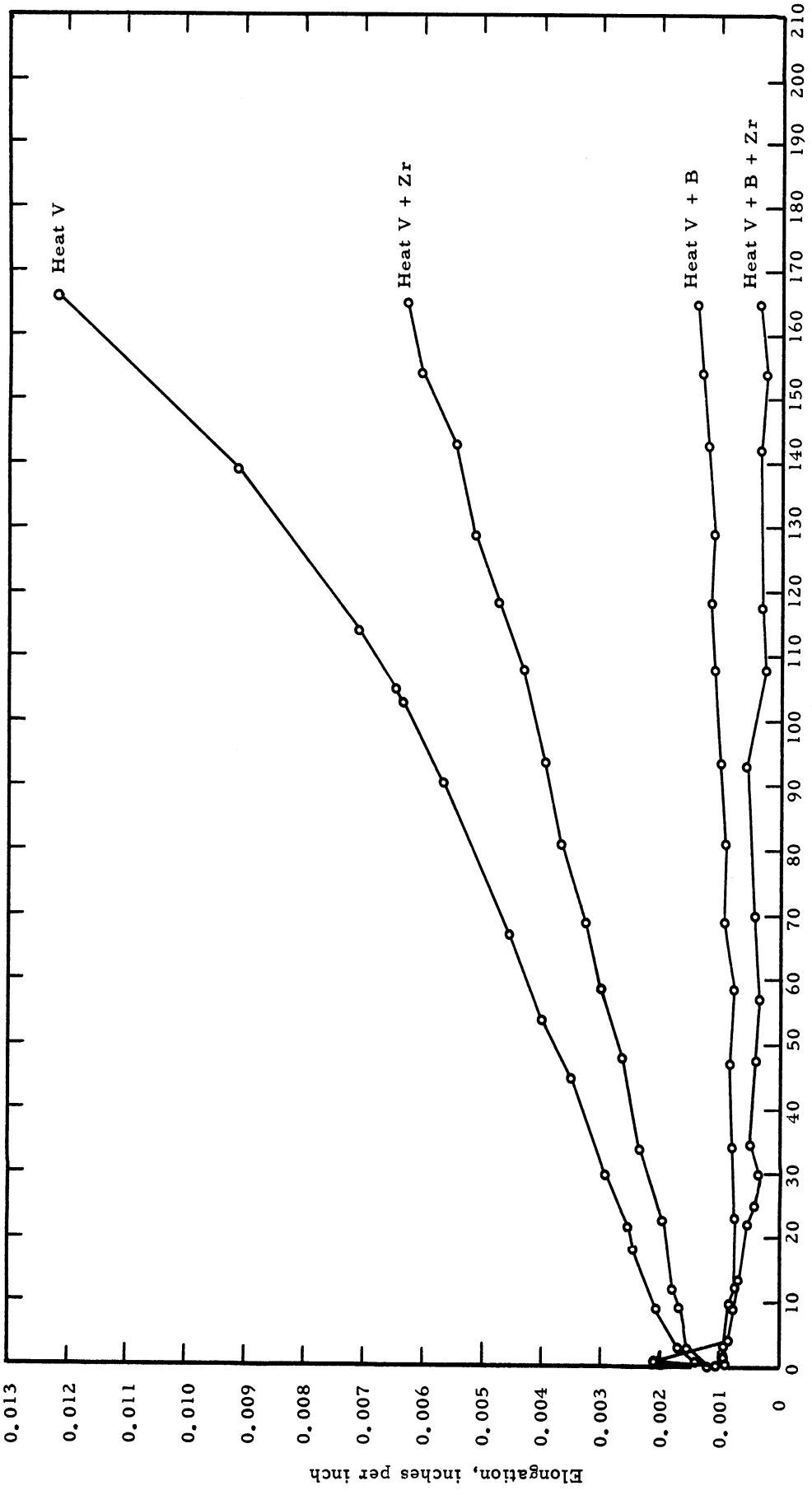

Figure 6. - Comparative creep curves at 1600°F and 20,000 psi for experimental heats.

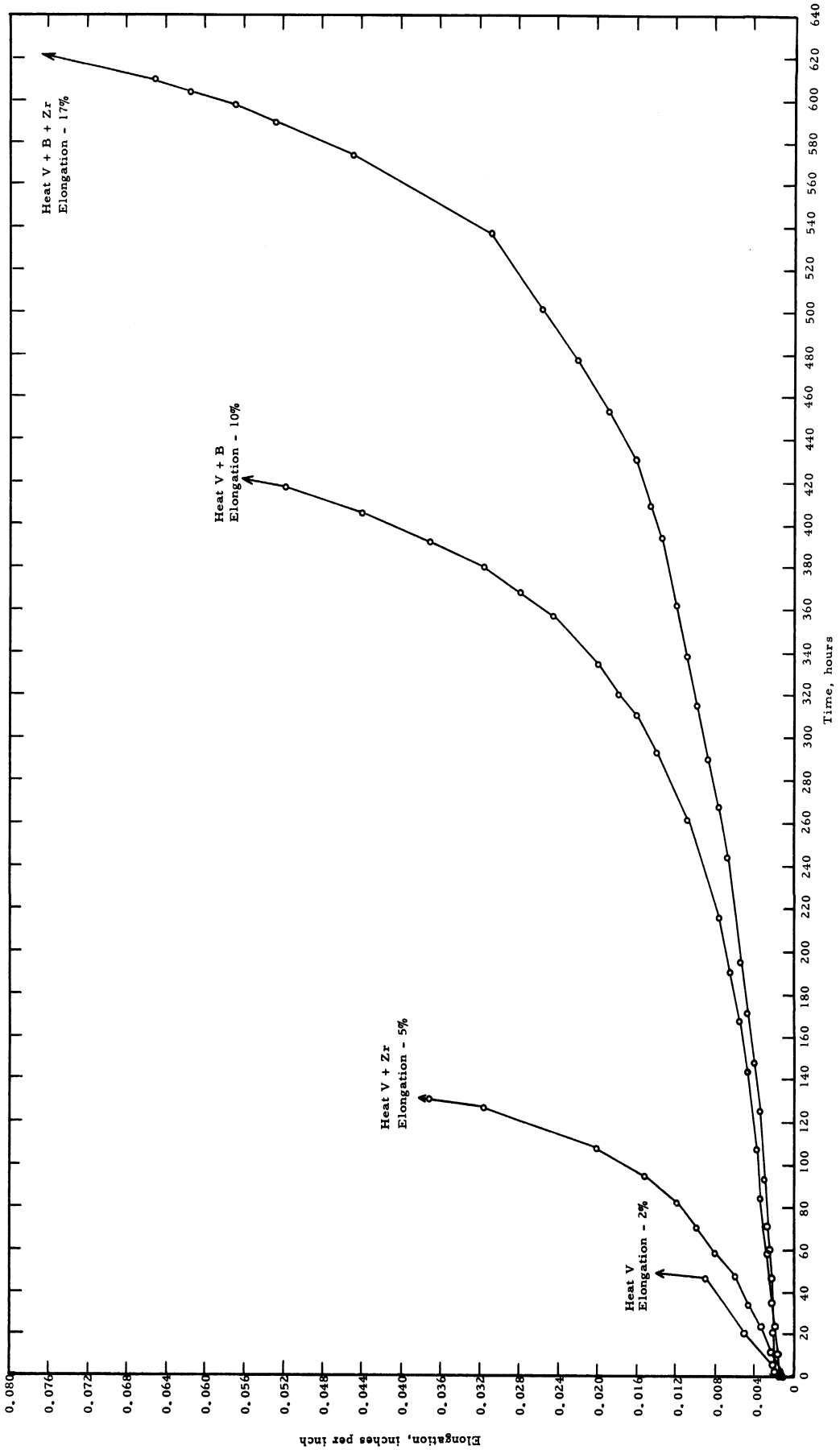

Figure 7. - Comparative creep curves at 1600°F and 25,000 psi for experimental heats.

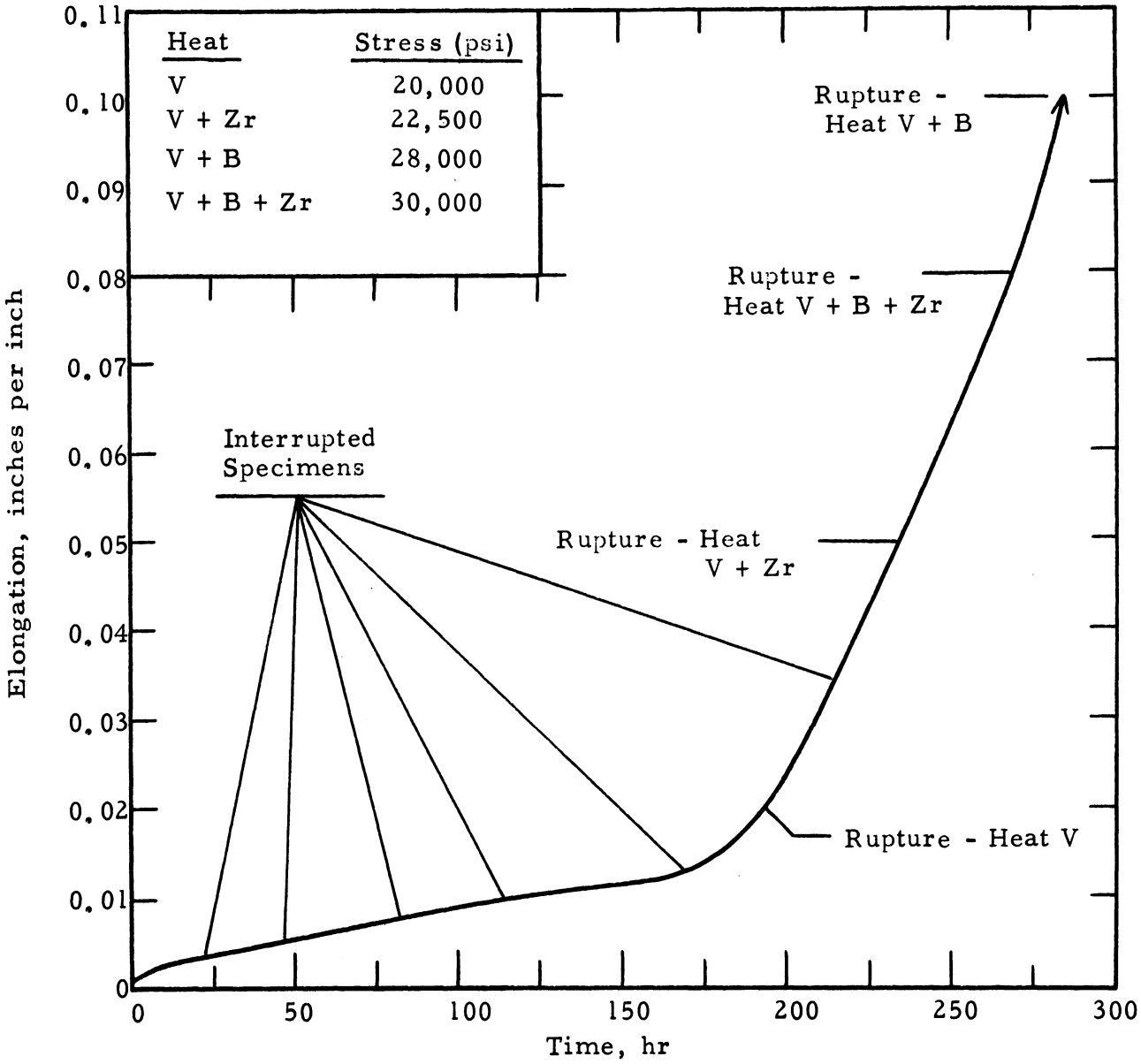

Figure 8. - Average creep curve of specimens stress aged to give equal creep deformations in equal time at 1600°F. Creep deformations at which specimens were interrupted or ruptured are indicated.

Heat V. DPH-354

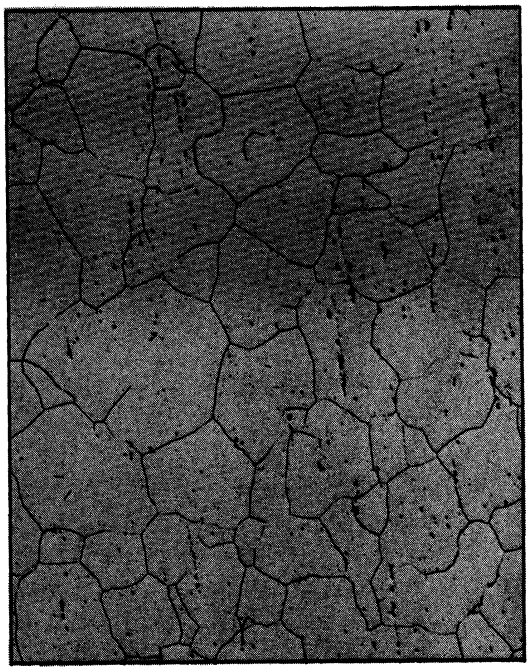

Heat V + Zr. DPH-353

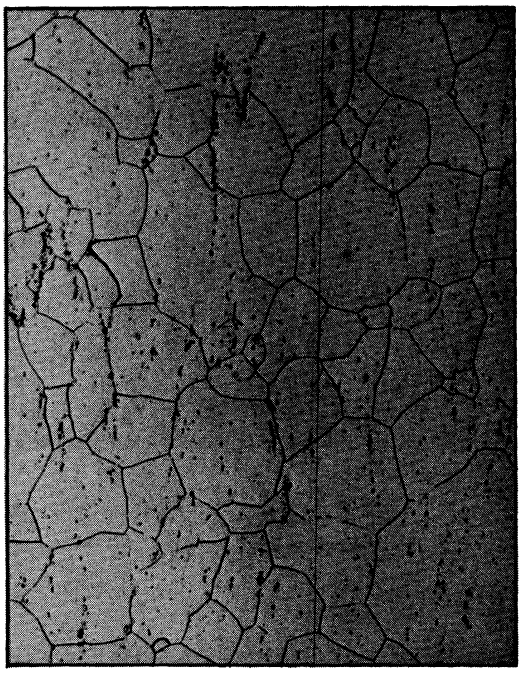

Heat V + B. DPH-345

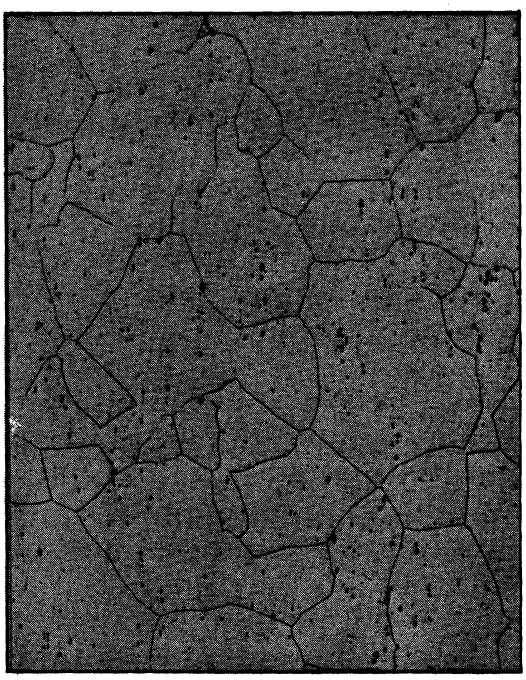

Heat V + B + Zr. DPH-348

Figure 9. - Initial condition of experimental heats as treated 2 hours at 2150°F, air cooled. X100D.

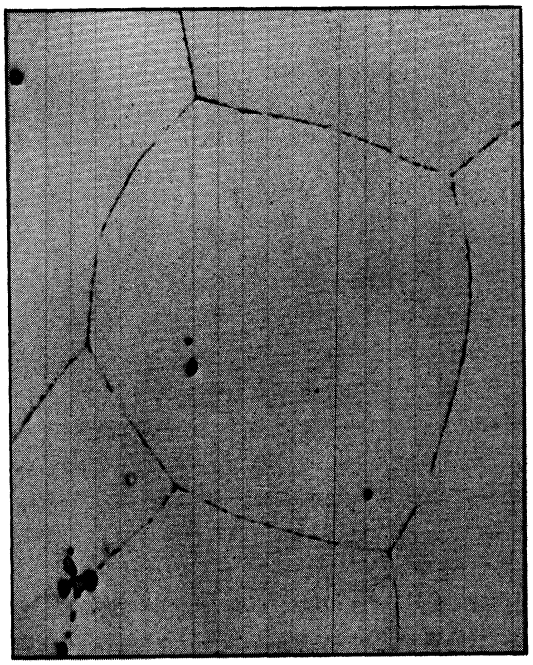

Heat V.

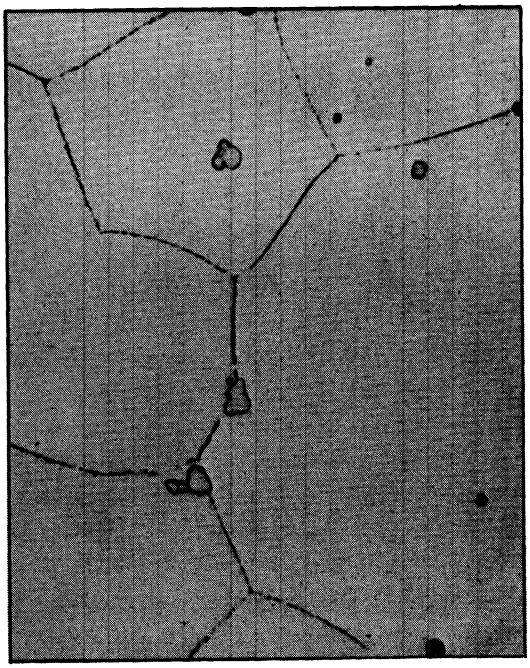

Heat V + Zr.

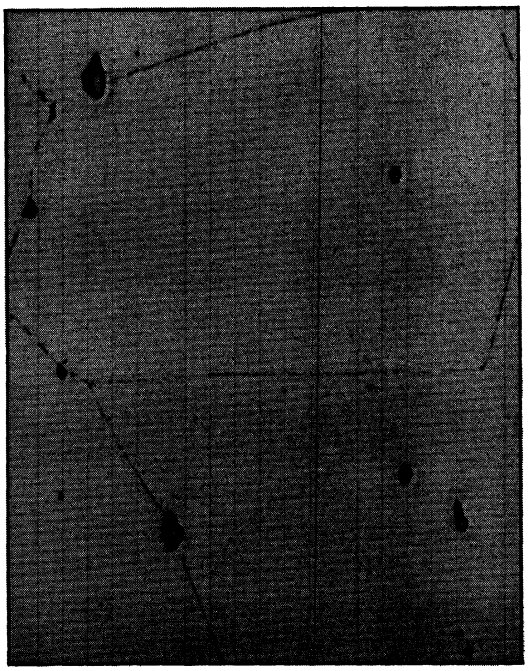

Heat V + B.

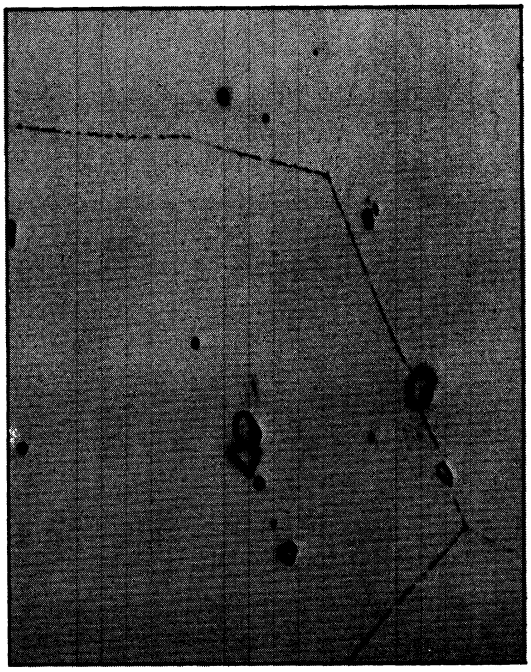

Heat V + B + Zr.

Figure 10. - Initial condition of experimental heats as treated 2 hours at 2150°F, air cooled. X1000D.

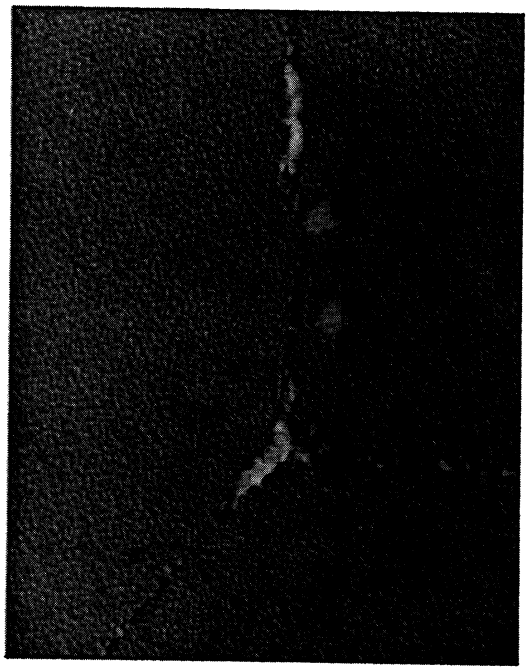

Heat V.

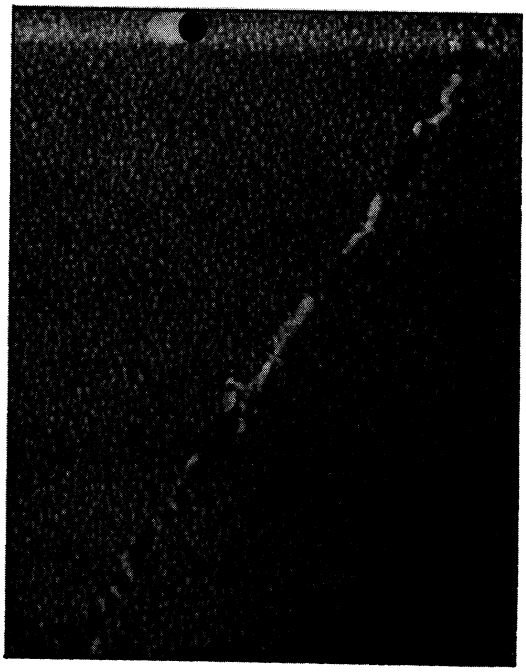

Heat V + Zr.

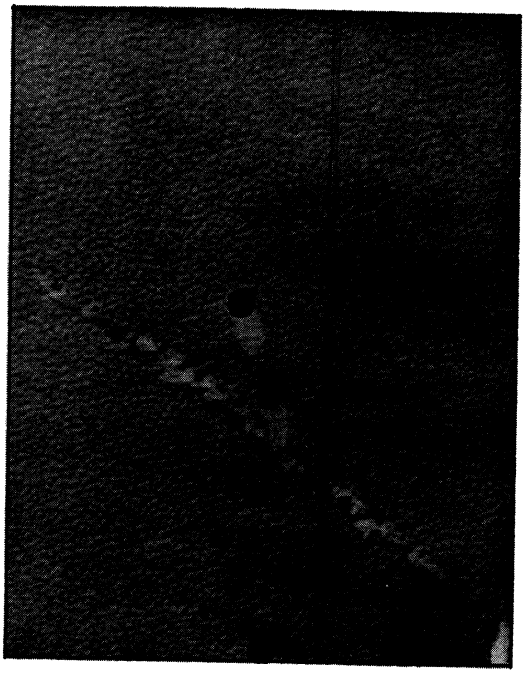

Heat V + B.

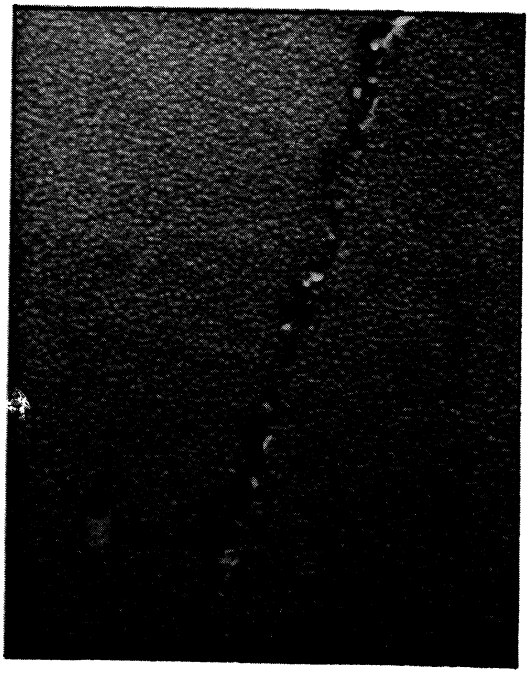

Heat V + B + Zr.

Figure 11. - Initial condition of experimental heats as treated 2 hours at 2150°F, air cooled. Electron micrographs X12,000D.

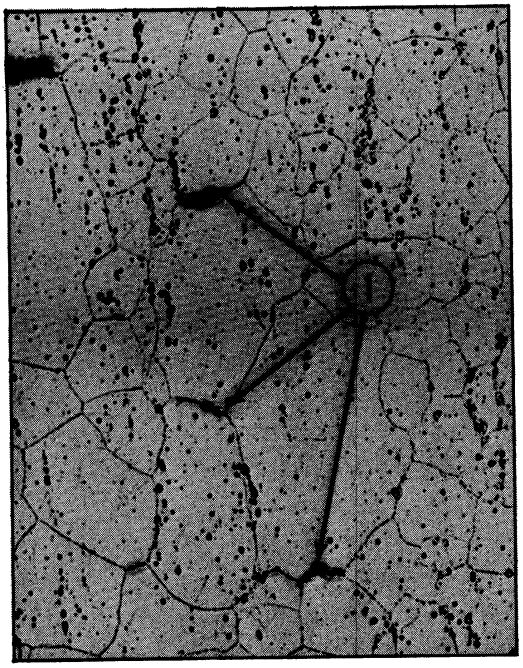

Heat V.

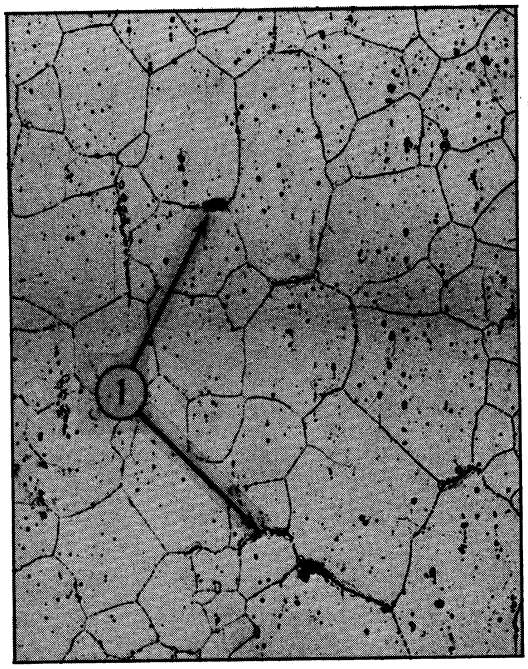

Heat V + Zr.

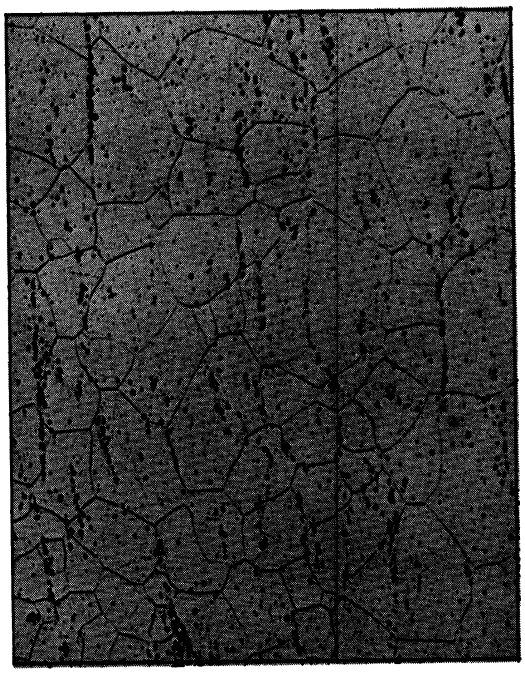

Heat V + B.

Heat V + B + Zr.

Figure 12. - Microstructures of experimental heats after 1.2 percent deformation by creep at 1600°F in 165-214 hours. Electropolished. X100D. ① - micro-crack.

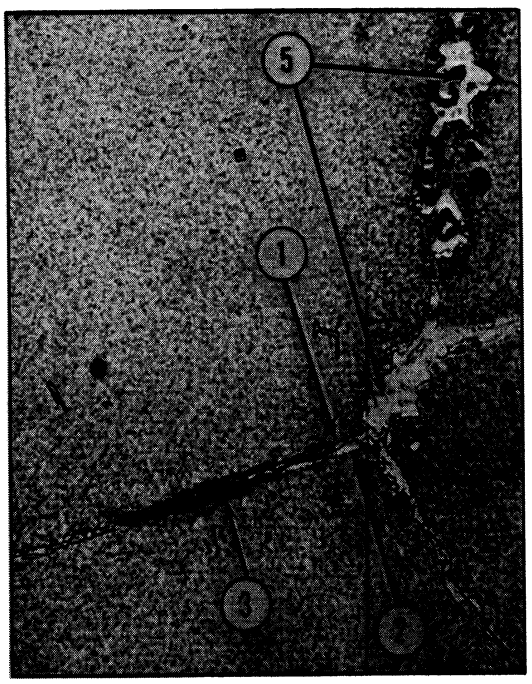

Heat V.

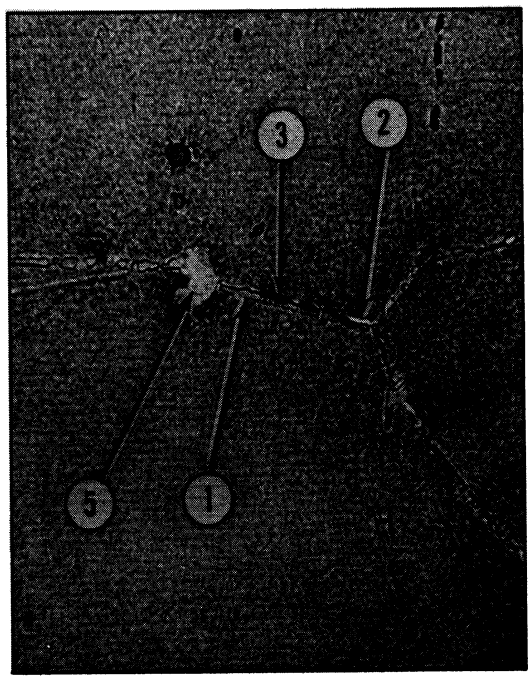

Heat V + Zr.

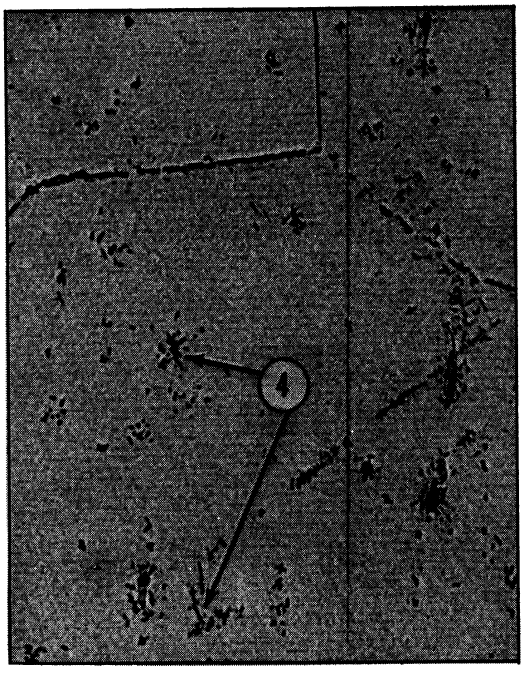

Heat V + B.

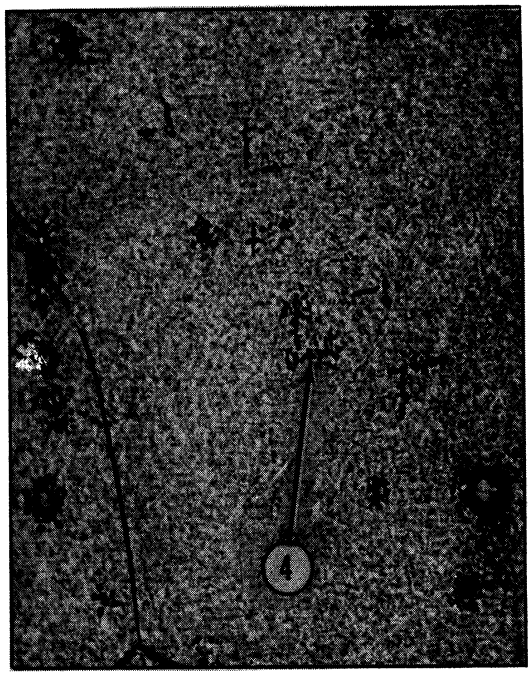

Heat V + B + Zr.

Figure 13. - Microstructures of experimental heats after 1.2 percent deformation by creep at 1600°F in 165-214 hours. X1000D. ① - intergranular $M_{23}C_6$; ② - depleted grain boundary; ③ - micro-crack; ④ - intragranular carbide; ⑤ - nodule.

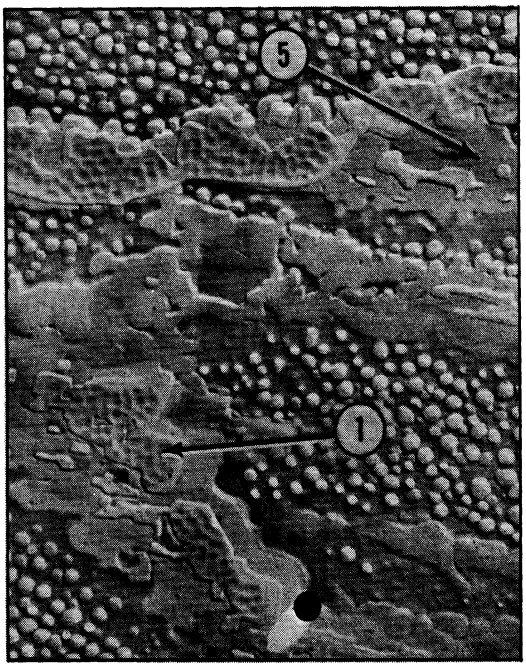

Heat V, typical grain boundaries.

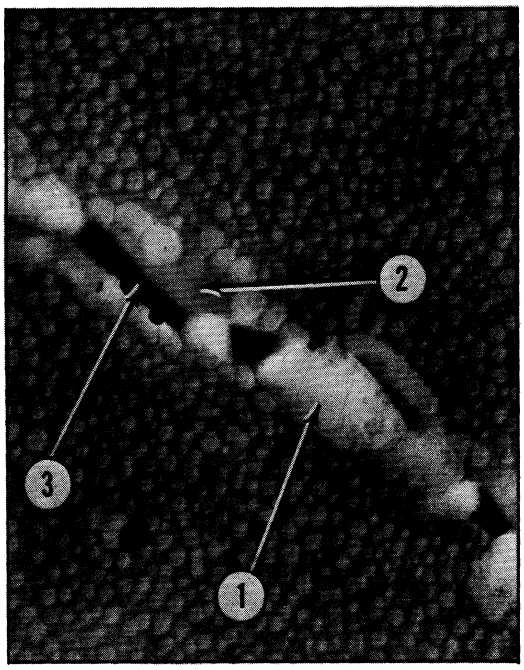

Heat V + Zr, depleted and cracked grain boundary with typical $M_{23}C_6$ precipitate.

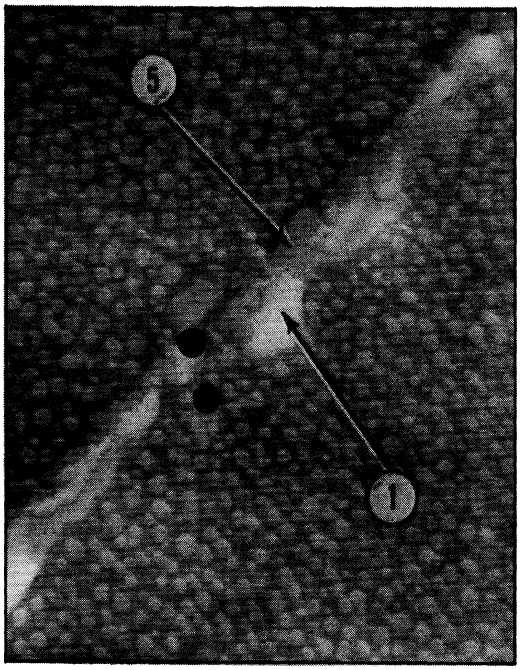

Heat V + B, typical grain boundary.

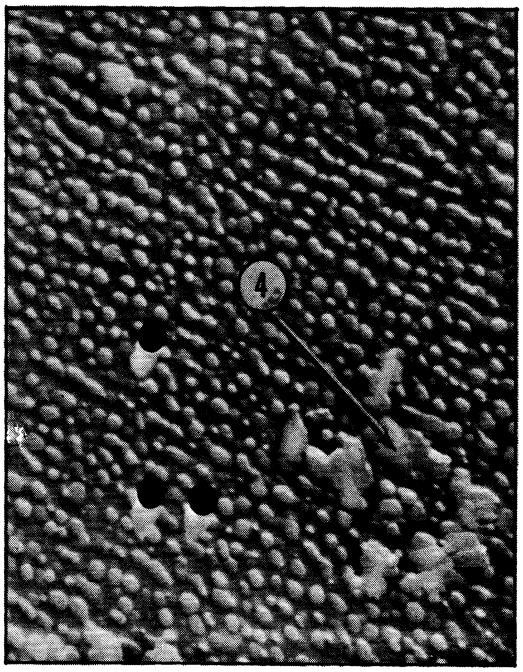

Heat V + B, intragranular carbides and alignment of γ'.

Figure 14. - Microstructures of experimental heats after 1.2 percent deformation by creep at 1600°F in 165-214 hours. Electron micrographs X12,000D. ① - intergranular $M_{23}C_6$; ② - depleted grain boundary; ③ - micro-crack; ④ - intragranular carbide; ⑤ - γ'; ⑥ - Ti(C,N).

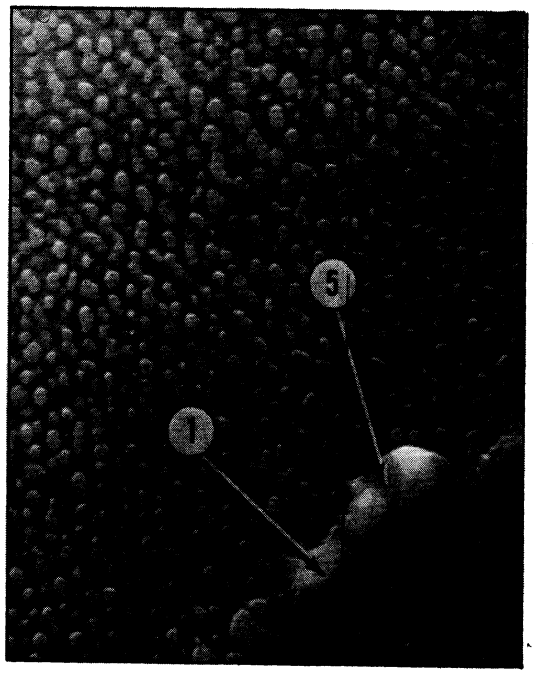

Heat V + B + Zr, typical grain boundary and alignment of γ'.

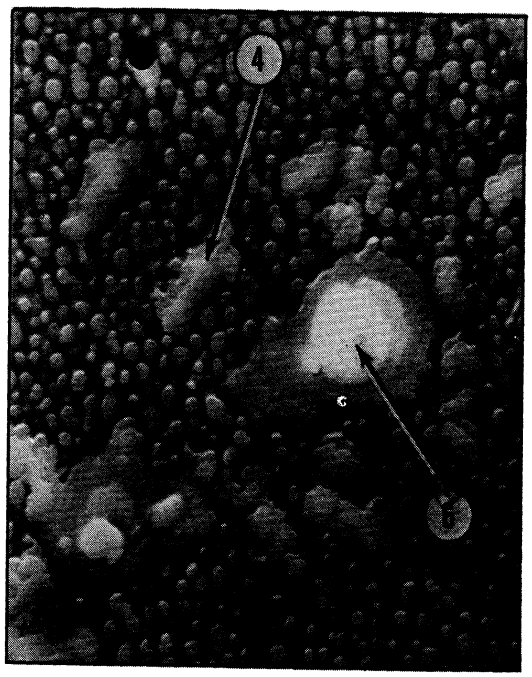

Heat V + B + Zr, intragranular carbides surrounding Ti(C,N).

Figure 14. - concluded.

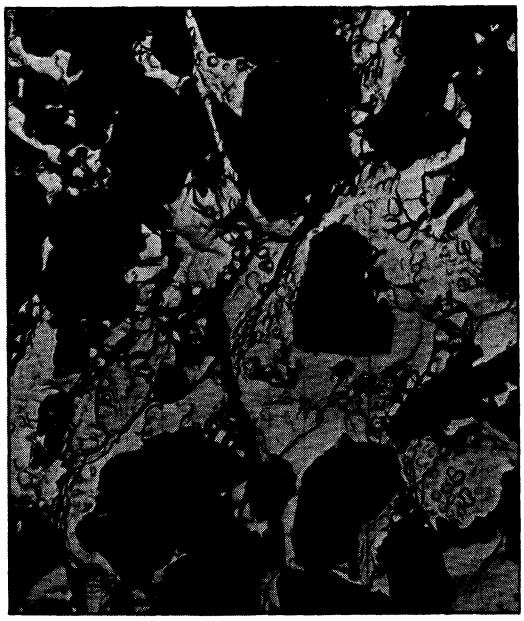

X8000D
Extraction replica of carbide from intergranular fracture surface of Heat V after 1.2 percent creep deformation in 165 hours at 1600°F. All selected area electron diffration spots indexed as $M_{23}C_6$.

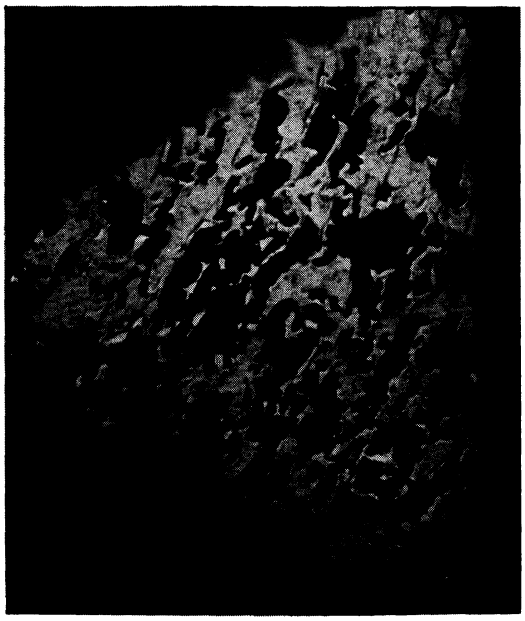

X8000D
Extraction replica of carbide from intergranular fracture surface of Heat V + B after 1.2 percent creep deformation in 188 hours at 1600°F. All selected area electron diffraction spots indexed as $M_{23}C_6$.

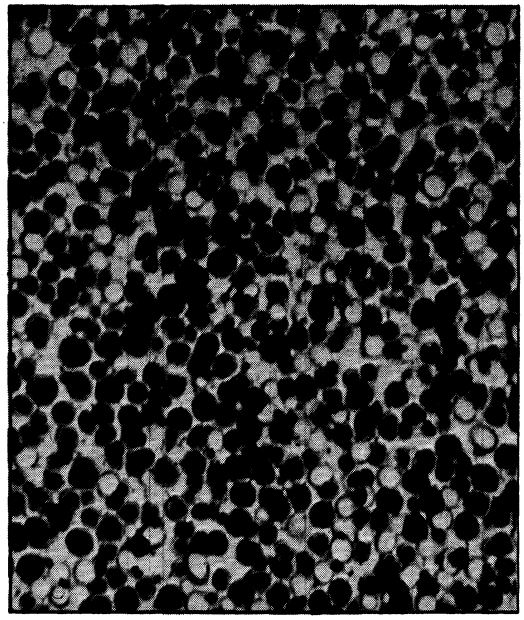

X36,000D
Extraction replica of intragranular γ' from Heat V + Zr after aging 10 hours at 1600°F. All selected area electron diffration spots indexed as γ'.

X8000D
Extraction replica of intragranular carbide from Heat V + B after 1.2 percent creep deformation in 188 hours at 1600°F. Most selected area electron diffraction spots indexed as M_6C; a few as $M_{23}C_6$.

Figure 15. - Micrographs of phases extracted from the experimental heats. Extracted particles appear black.

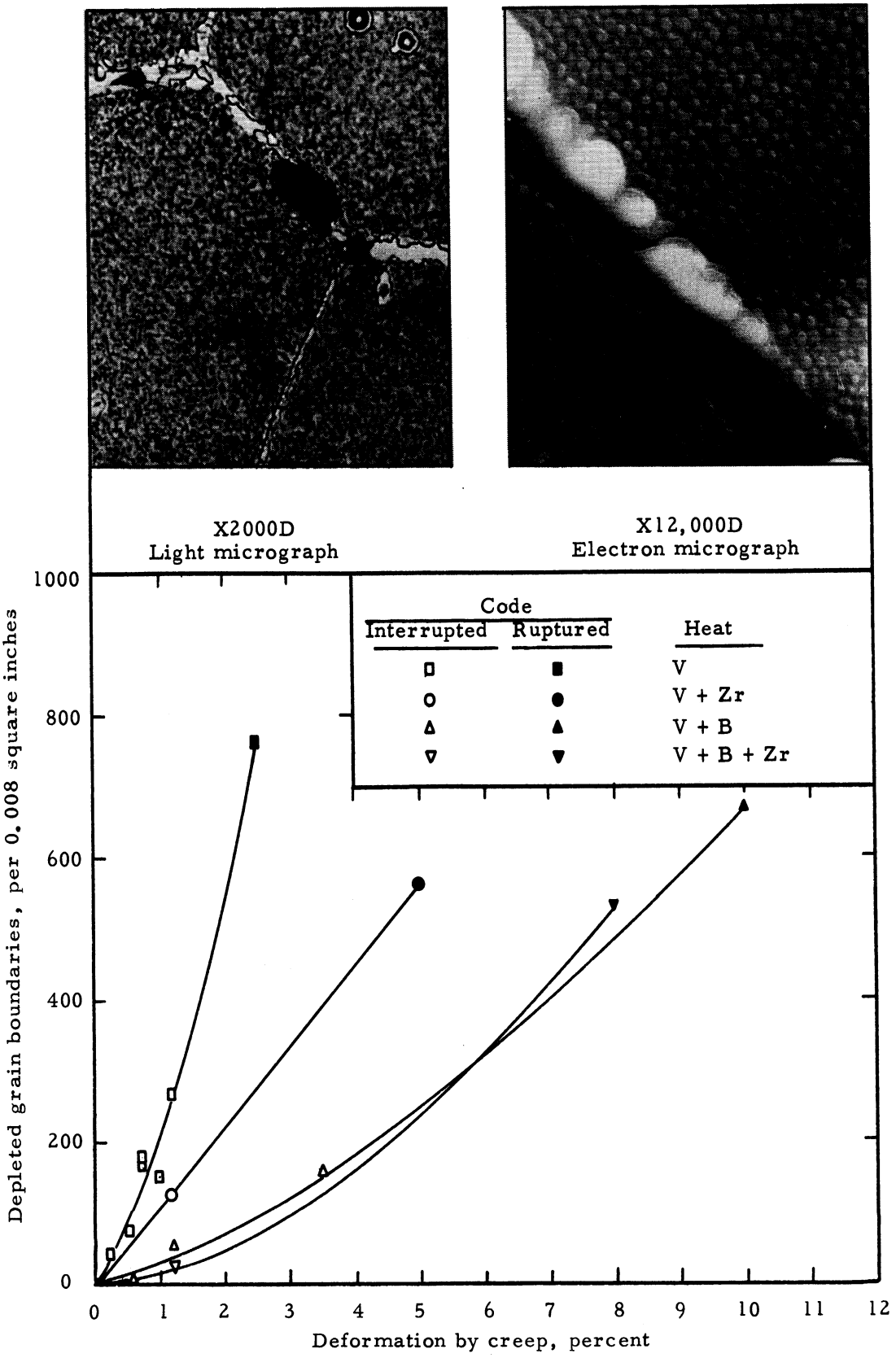

Figure 16. - Effect of creep deformation at 1600°F on depletion of grain boundaries of experimental heats. Stressed to give comparable strain rates. Micrographs of typical depleted grain boundaries are shown for electropolished specimen.

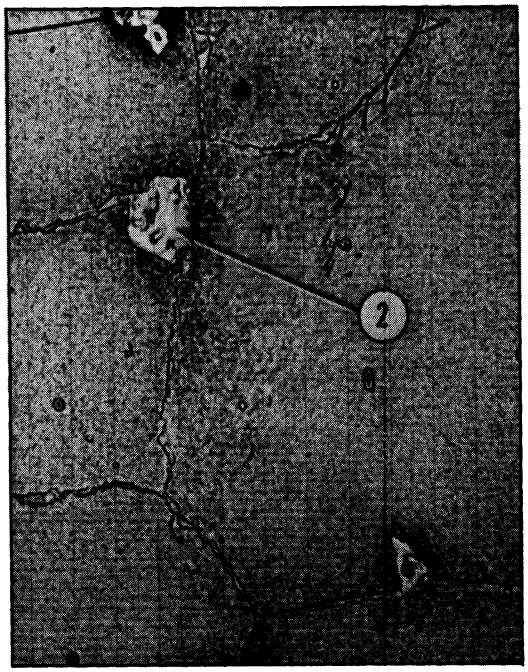

Heat V. DPH-338

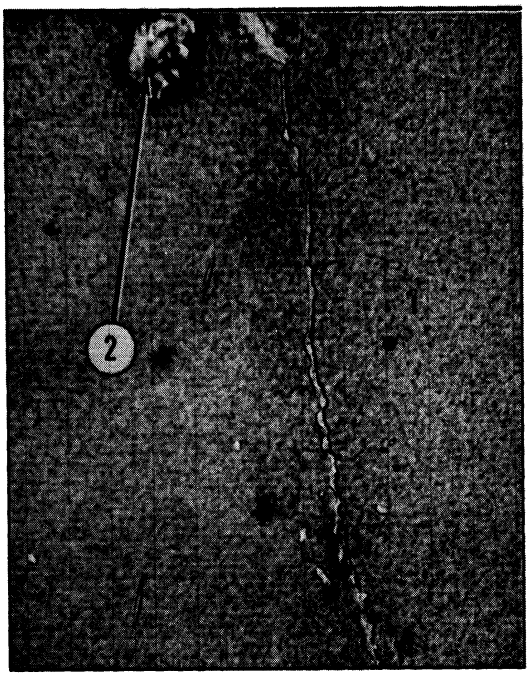

Heat V + Zr. DPH-342

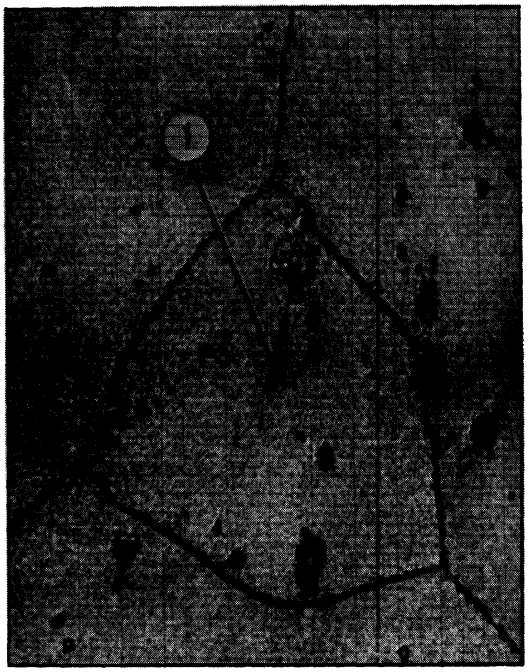

Heat V + B. DPH-340

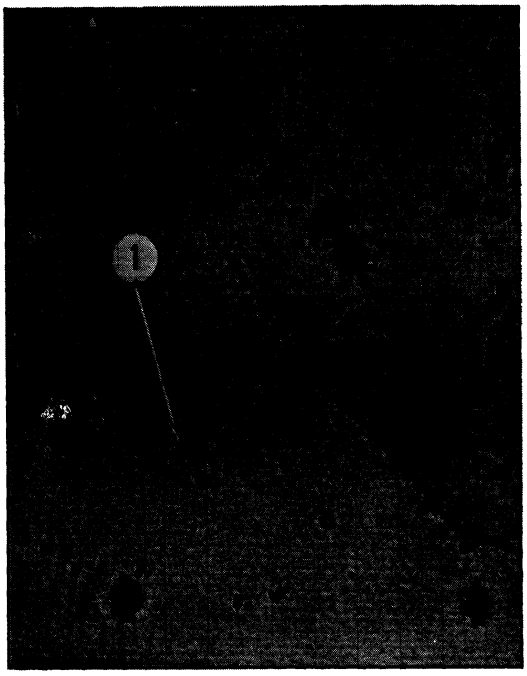

Heat V + B + Zr DPH-353

Figure 17. - Microstructures of experimental heats after aging 188 hours at 1600°F. X 1000D. ① - intragranular carbide; ② - nodule.

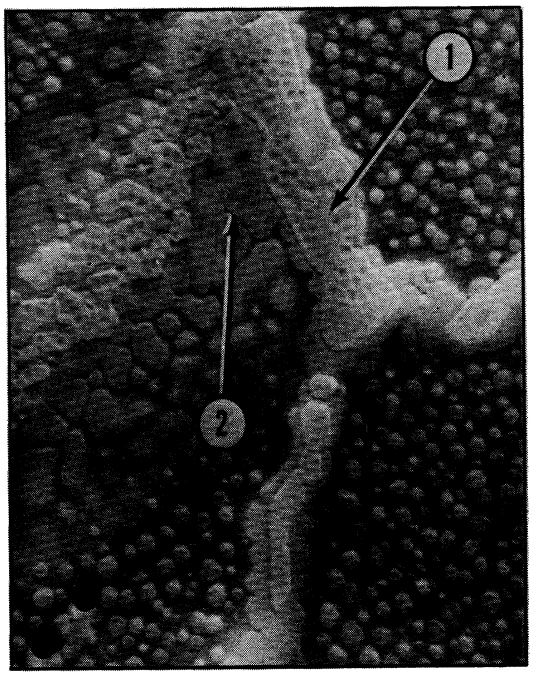

Heat V.

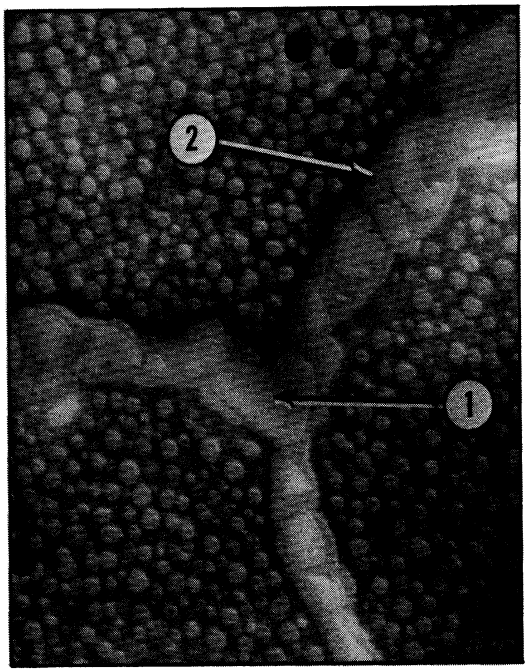

Heat V + Zr.

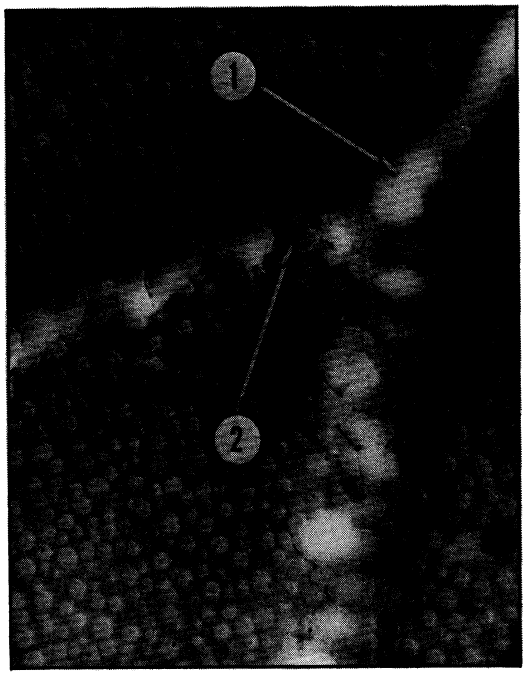

Heat V + B.

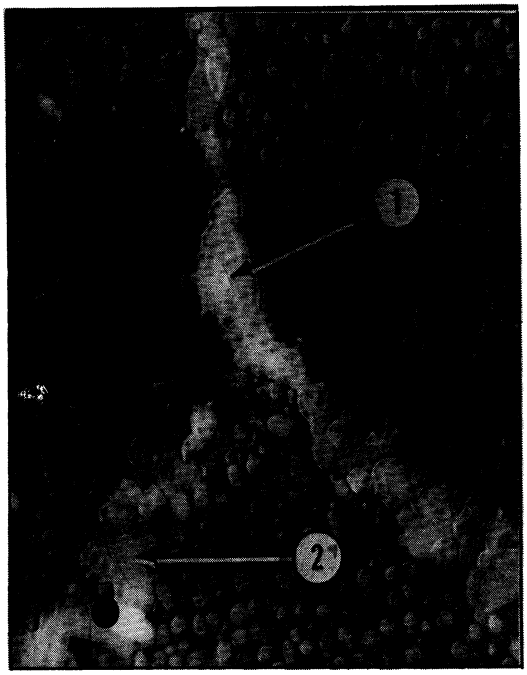

Heat V + B + Zr.

Figure 18. - Microstructures of experimental heats after aging 188 hours at 1600°F. Electron micrographs X12,000D. ① - intergranular $M_{23}C_6$; ② - γ'.

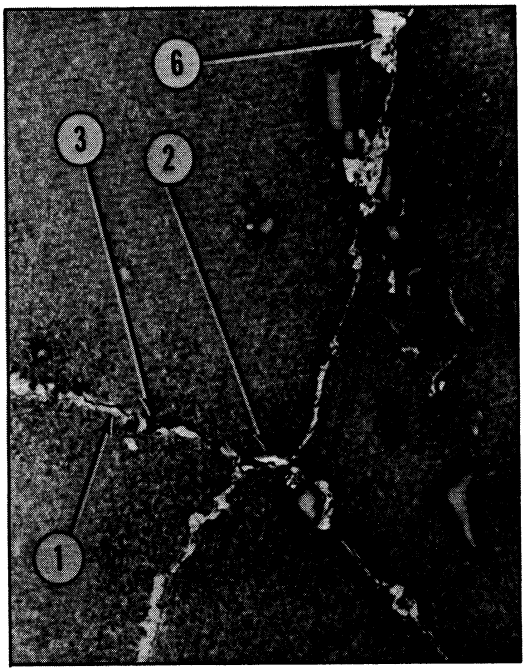

Heat V.

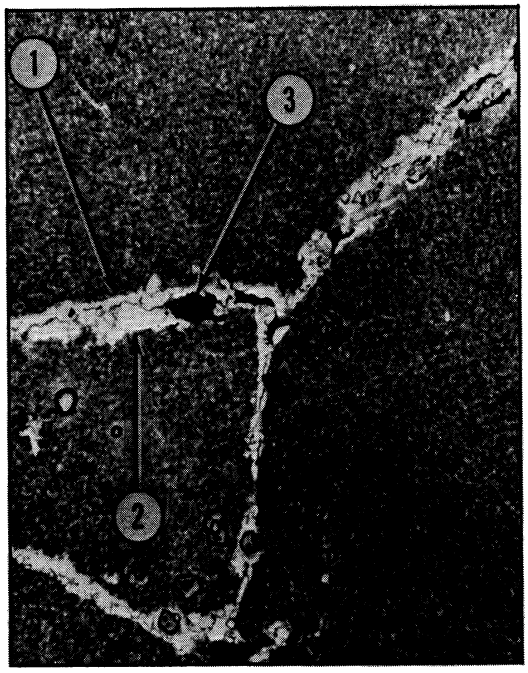

Heat V + Zr.

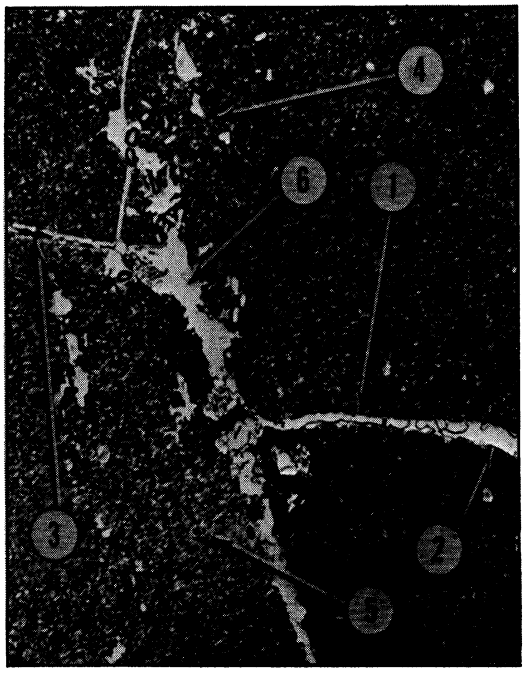

Heat V + B.

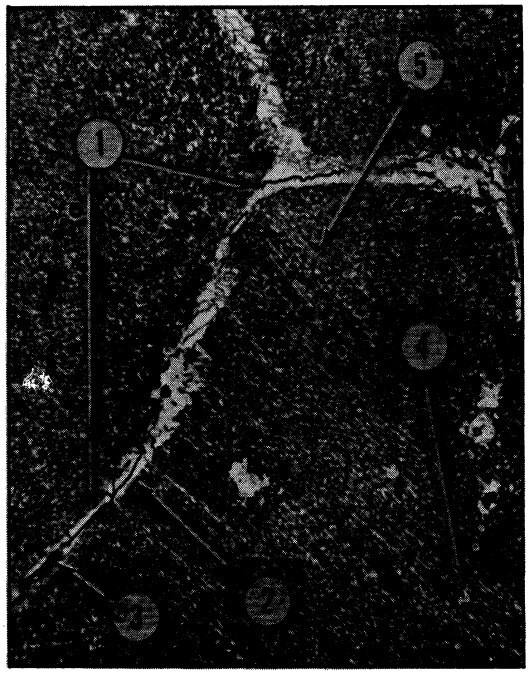

Heat V + B + Zr.

Figure 19. - Microstructures of experimental heats after rupture at 1600°F and 25,000 psi. X1000D. ① - intergranular $M_{23}C_6$; ② - depleted grain boundary; ③ - micro-crack; ④ - intragranular carbide; ⑤ - alignment of γ'; ⑥ - nodule.

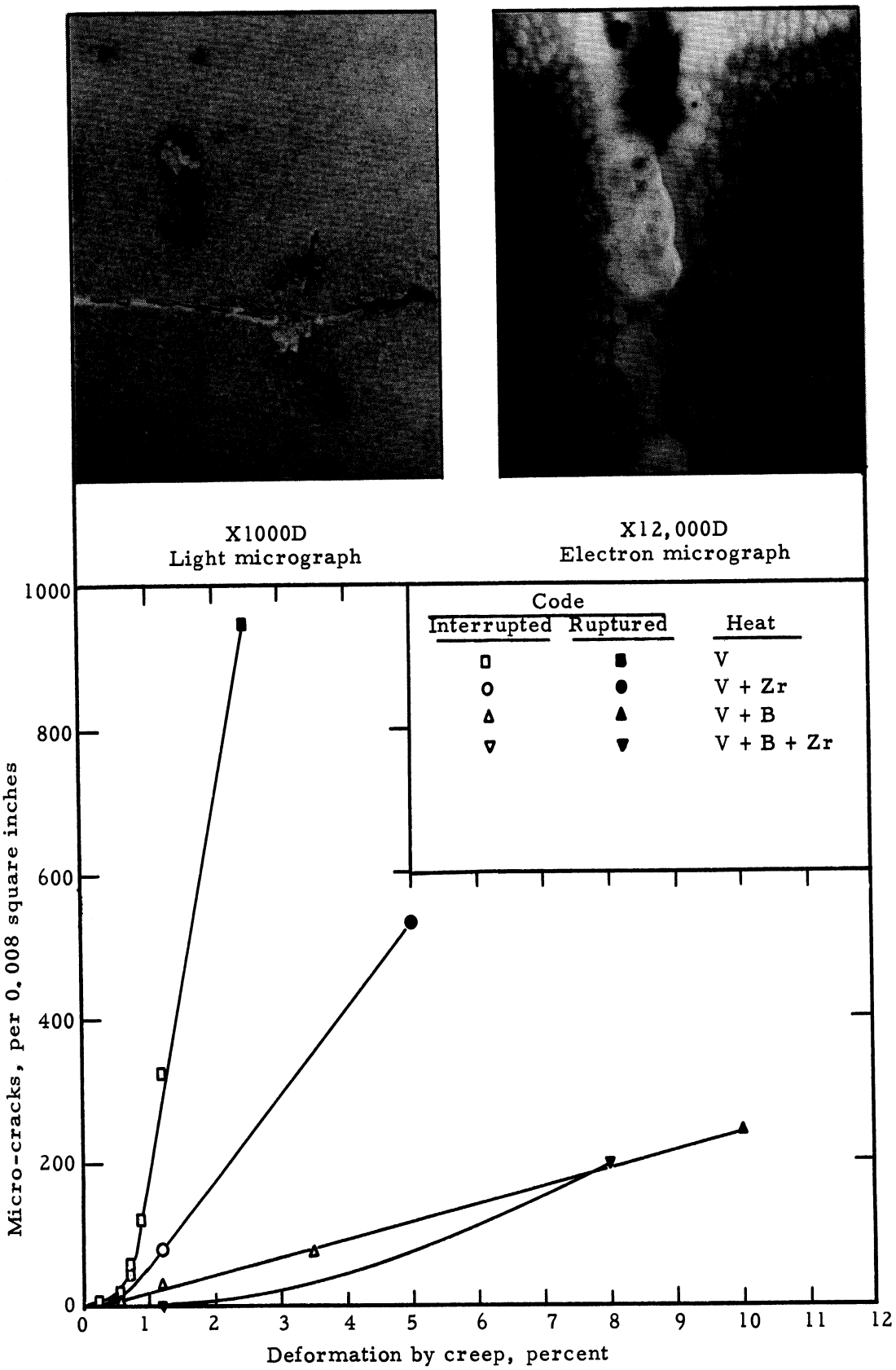

Figure 20. - Effect of creep deformation at 1600°F on micro-cracking of experimental heats. Stressed to give comparable strain rates. Micrographs of typical micro-cracks are shown. Tension axis is horizontal in the electron micrograph.

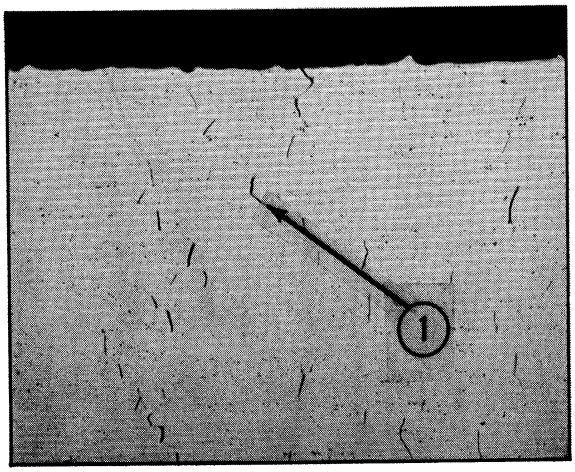

Heat V, ruptured in 52 hours at 1600°F and 25,000 psi with 13 surface cracks and 376 micro-cracks.

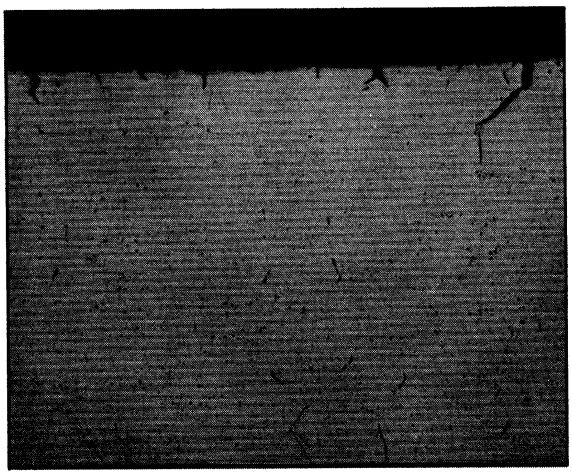

Heat V + B, ruptured in 296 hours at 1600°F and 28,000 psi with 160 surface cracks and 243 micro-cracks.

Heat V + B + Zr, ruptured in 266 hours at 1600°F and 30,000 psi with 300 surface cracks and 198 micro-cracks.

Figure 21. - Change in mode of cracking in experimental heats. Surface cracks are number per inch of transverse section penetrating more than 0.003 inch. Micro-cracks are number in 0.008 square inches observed. X32D. ① - micro-crack; ② - surface cracks.

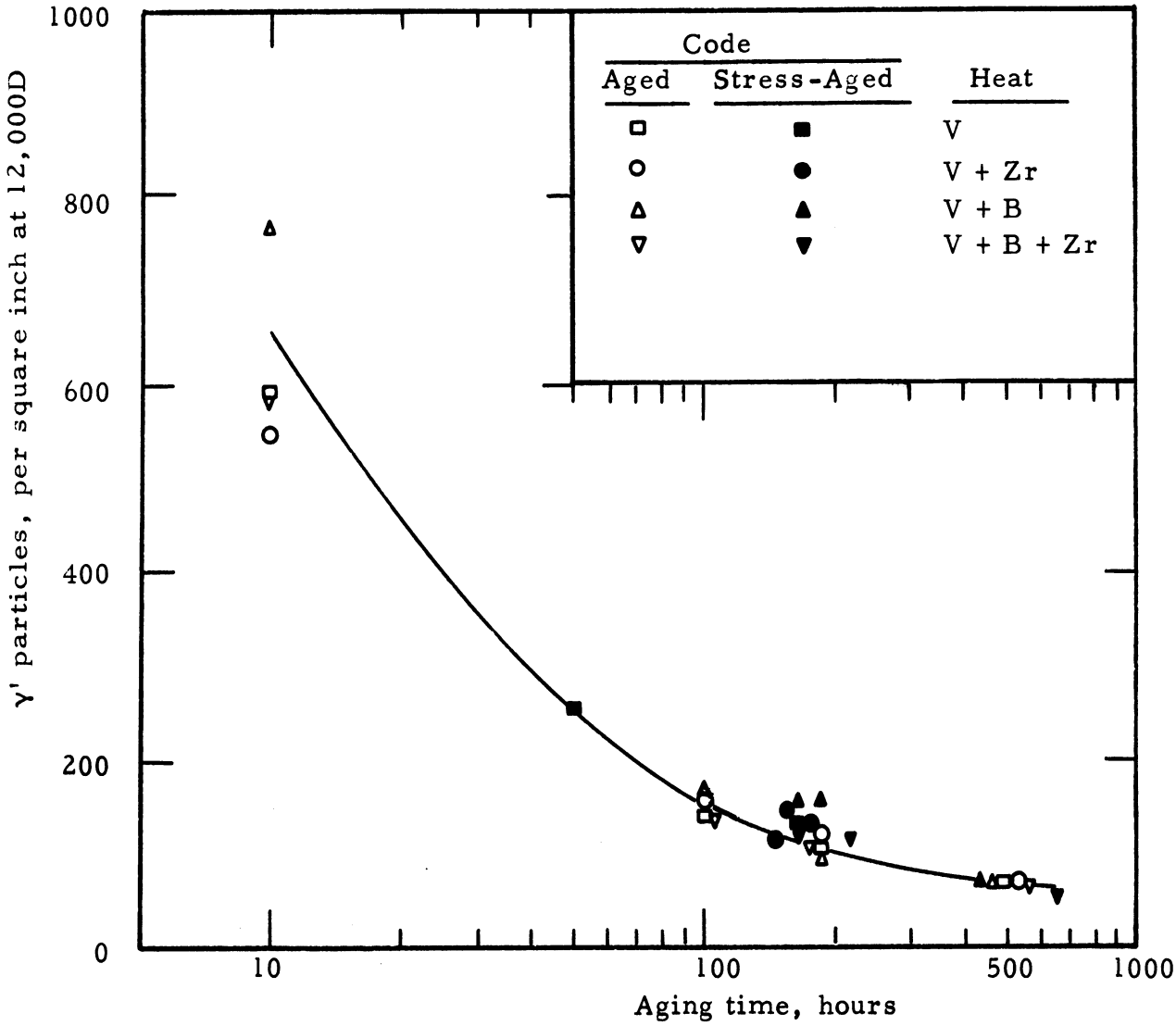

Figure 22. - Effect of aging time at 1600°F on γ' particle density in experimental heats. Stress aging was at 20,000 - 30,000 psi.

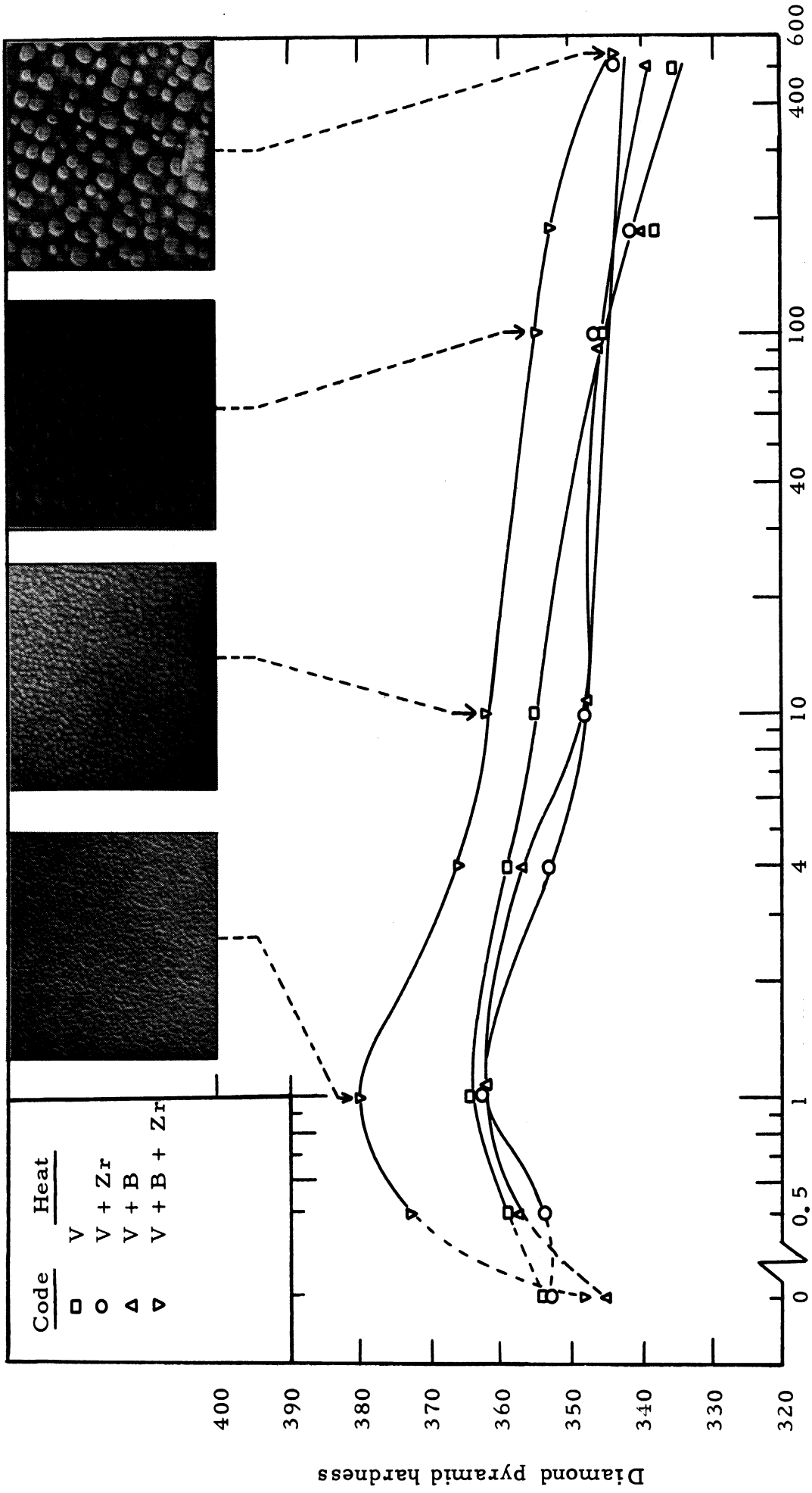

Figure 23. - Effect of aging at 1600°F on hardness and γ' dispersion of experimental heats. Typical electron micrographs at 12,000D are shown.

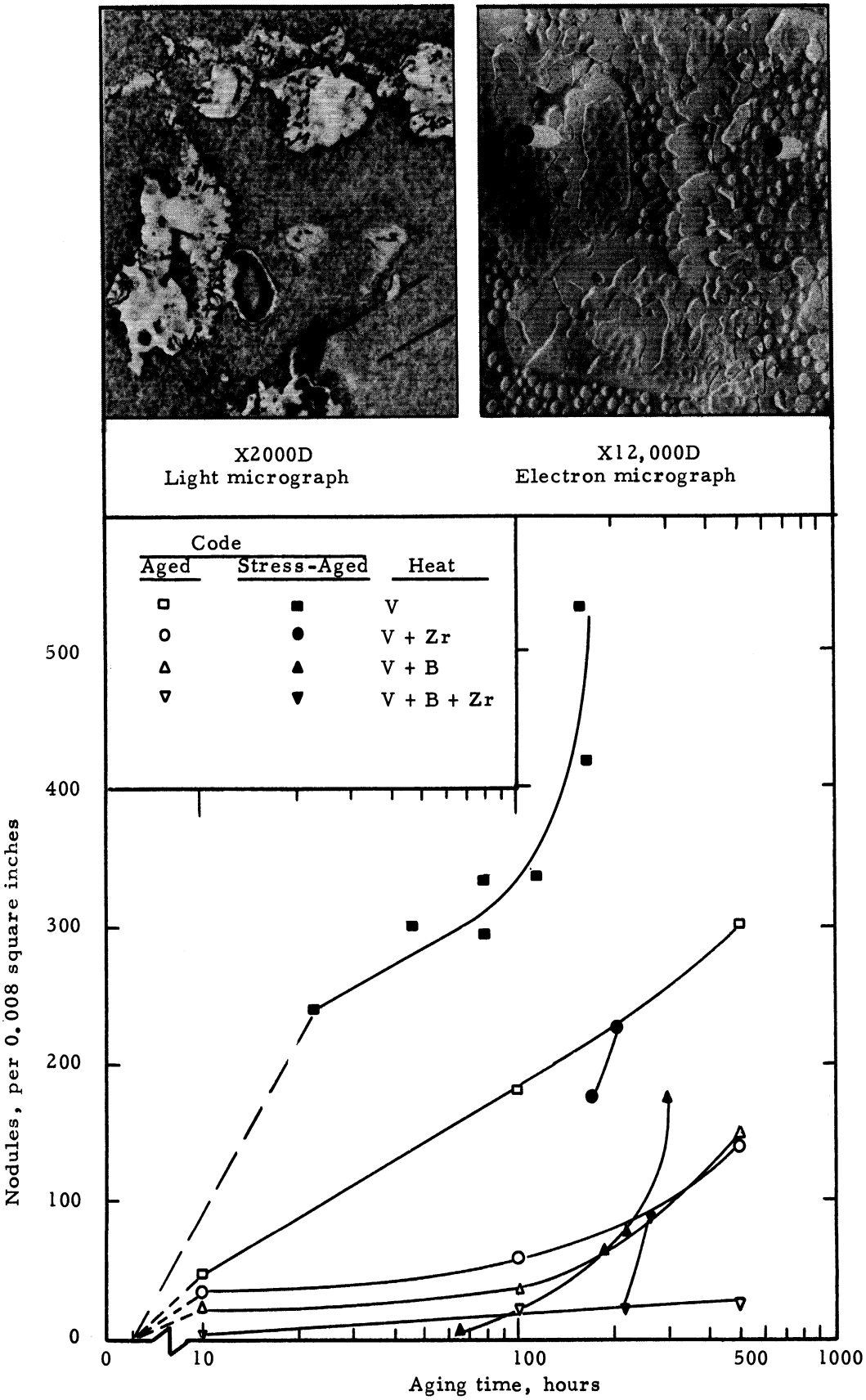

Figure 24. - Effect of aging time at 1600°F on nodule density of experimental heats. Stress aging was at comparable strain rates. Micrographs of typical nodules are shown.

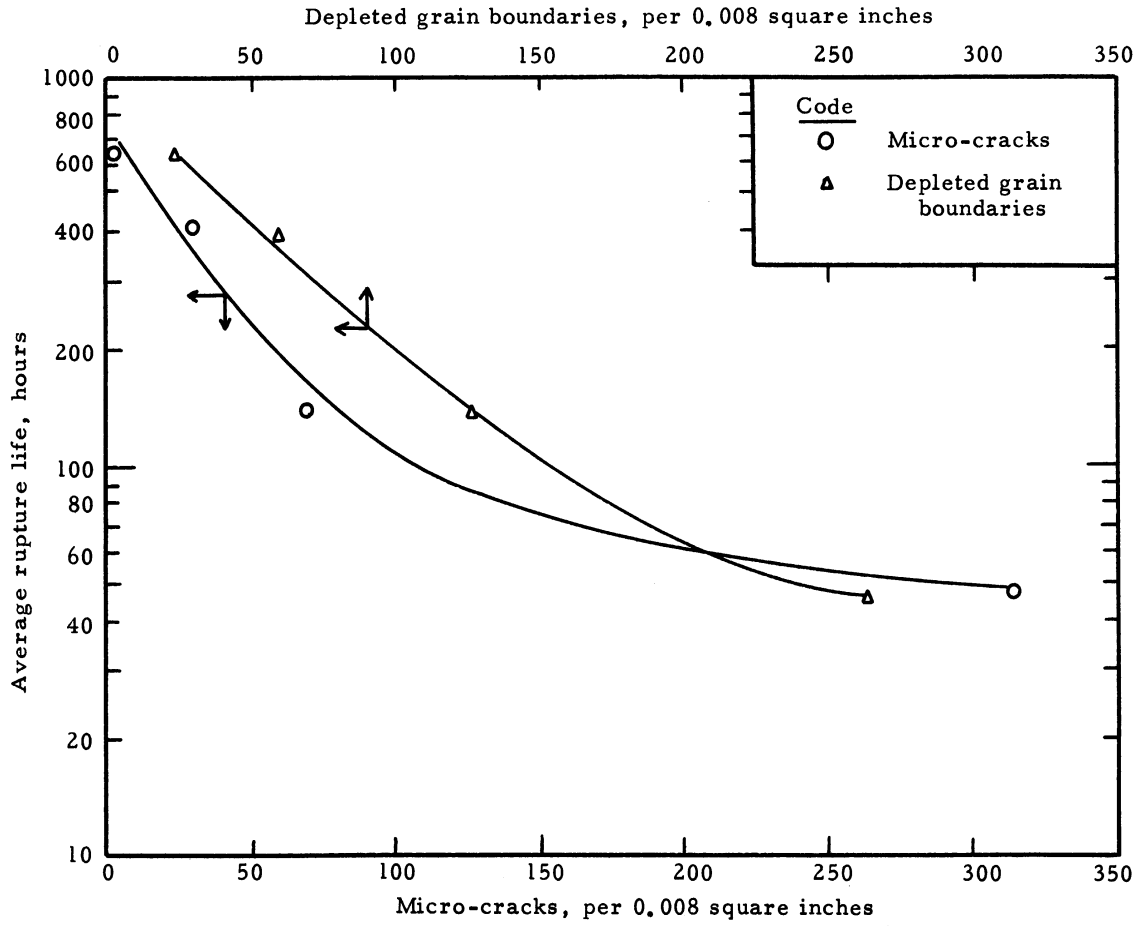

Figure 25. - Relation of rupture life at 1600°F and 25,000 psi to micro-cracking and depletion tendencies of experimental heats when stressed to give 1.2% deformation in 165 - 214 hours.

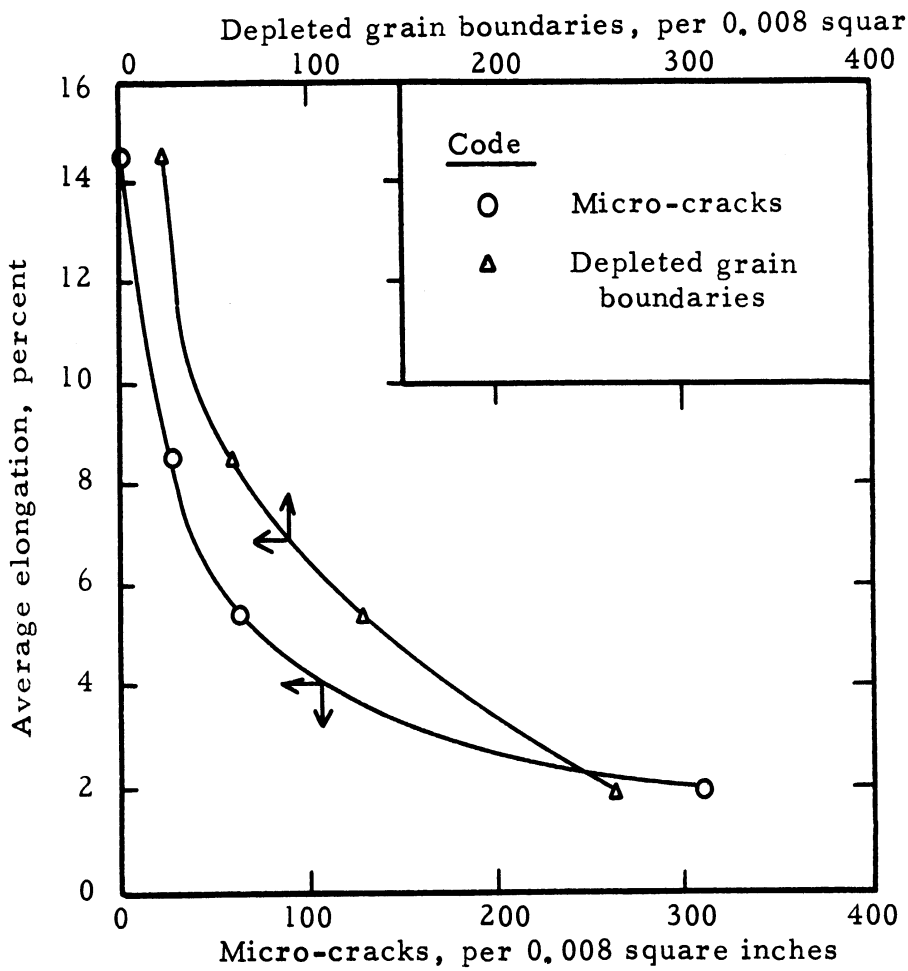

Figure 26. - Relation of elongation at 1600°F and 25,000 psi to micro-cracking and depletion tendencies of experimental heats when stressed to give 1.2% deformation in 165-214 hours.